Simulating the vegetation response in western Europe to abrupt climate changes under glacial background conditions

M.-N. Woillez, M. Kageyama, N. Combourieu-Nebout, G. Krinner

Biogeosciences, 10, 1561–1582, 2013
www.biogeosciences.net/10/1561/2013/
doi:10.5194/bg-10-1561-2013

Biogeosciences Open Access

Simulating the vegetation response in western Europe to abrupt climate changes under glacial background conditions

M.-N. Woillez[1], **M. Kageyama**[1], **N. Combourieu-Nebout**[1], **and G. Krinner**[2]

[1]LSCE/IPSL INSU, CEA-CNRS-UVSQ UMR8212, CE Saclay, l'Orme des Merisiers, 91191 Gif-sur-Yvette Cedex, France
[2]LGGE, CNRS UMR5183, 54 rue Molière, 38402 St. Martin d'Hères Cedex, France

Correspondence to: M.-N. Woillez (marie-noelle.woillez@lsce.ipsl.fr)

Received: 9 August 2012 – Published in Biogeosciences Discuss.: 19 September 2012
Revised: 21 December 2012 – Accepted: 31 January 2013 – Published: 7 March 2013

Abstract. The last glacial period has been punctuated by two types of abrupt climatic events, the Dansgaard–Oeschger (DO) and Heinrich (HE) events. These events, recorded in Greenland ice and in marine sediments, involved changes in the Atlantic Meridional Overturning Circulation (AMOC) and led to major changes in the terrestrial biosphere.

Here we use the dynamical global vegetation model ORCHIDEE to simulate the response of vegetation to abrupt changes in the AMOC strength. We force ORCHIDEE offline with outputs from the IPSL_CM4 general circulation model, in which the AMOC is forced to change by adding freshwater fluxes in the North Atlantic. We investigate the impact of a collapse and recovery of the AMOC, at different rates, and focus on Western Europe, where many pollen records are available for comparison.

The impact of an AMOC collapse on the European mean temperatures and precipitations simulated by the GCM is relatively small but sufficient to drive an important regression of forests and expansion of grasses in ORCHIDEE, in qualitative agreement with pollen data for an HE event. On the contrary, a run with a rapid shift of the AMOC to a hyperactive state of 30 Sv, mimicking the warming phase of a DO event, does not exhibit a strong impact on the European vegetation compared to the glacial control state. For our model, simulating the impact of an HE event thus appears easier than simulating the abrupt transition towards the interstadial phase of a DO.

For both a collapse or a recovery of the AMOC, the vegetation starts to respond to climatic changes immediately but reaches equilibrium about 200 yr after the climate equilibrates, suggesting a possible bias in the climatic reconstructions based on pollen records, which assume equilibrium between climate and vegetation. However, our study does not take into account vegetation feedbacks on the atmosphere.

1 Introduction

The last glacial period (10–90 ky BP) has been punctuated by two types of abrupt climatic changes, the Dansgaard–Oeschger (DO) events (Dansgaard et al., 1993) and Heinrich events (Heinrich, 1988). The DO events are characterized by an initial abrupt warming of up to 8 to 16 °C over Greenland in a few decades (Johnsen et al., 1992, 1995; Landais et al., 2004; Wolff et al., 2010), followed by a warm phase (interstadial) during which the temperature gradually decreases over several hundred to several thousand years , ended by an abrupt return to cold conditions (stadial). Some of the stadials correspond to Heinrich events (HE), which are defined as massive iceberg discharges from the Laurentide ice sheet in the North Atlantic, occurring every 5 to 7 ky and recorded in marine sediment cores by the presence of ice-rafted detritus (Heinrich, 1988; Bond and Lotti, 1995). DO events apparently occurred with a periodicity of around 1500 yr (Alley et al., 2001; Schulz, 2002), however the significance of this periodicity is debated and some authors claim that the recurrence actually cannot be distinguished from a random occurrence (Ditlevsen et al., 2007).

The analysis of $\delta^{13}C$ in marine sediment cores shows a strong decrease in the strength of the Atlantic Meridional Overturning Circulation (AMOC) during the Heinrich events (e.g. Elliot et al., 2002), a result consistent with freshwater inputs in the North Atlantic from the melting of icebergs released by the adjacent ice sheets. Temperature

reconstructions from Antarctica show smaller and more gradual fluctuations, approximately out of phase with the Greenland temperature records (Jouzel et al., 2003; Blunier et al., 1998; EPICA Community Members, 2006). Abrupt changes opposite to the North Atlantic signal are recorded in the South Atlantic, at the present-day northern margin of the Antarctic Circumpolar Current (Barker et al., 2009). This opposite behaviour of the two hemispheres, called "bipolar see-saw" (Crowley, 1992; Stocker and Johnsen, 2003), has been explained by a reduction of the northward heat transport when the AMOC slows down, leading to a cooling of the Northern Hemisphere and to a warming of the Southern Hemisphere. The mechanism has been confirmed by many modelling studies which successfully reproduced the bipolar see-saw pattern when the AMOC collapses (see the reviews of Clement and Peterson, 2008 and Kageyama et al., 2010).

Contrary to HE events, the shift from a stadial to an interstadial state during a DO event does not seem to be associated with strong changes in the AMOC (Elliot et al., 2002). The modelling study by Ganopolski and Rahmstorf (2001) suggests that DO events are caused by shifts between two different modes of convection of the AMOC, driven by small fluctuations of the freshwater flux. It has been suggested that such fluctuations could be triggered by changes in solar irradiance (Braun et al., 2005), which could impact the ablation rate of the ice sheets (Woillez et al., 2012). However, so far, the ultimate cause of DO events remains an open issue.

Pollen records from marine and terrestrial cores reveal abrupt vegetation changes around the whole North Atlantic region, that can be correlated to DO and HE events. In Florida, records from Lake Tulane show an antiphase relationship with the North Atlantic region: oak-scrub and prairie vegetation during interstadials and the development of pine forest during stadials (Grimm et al., 2006), indicating a wetter and warmer climate for the stadials. In Western Europe, millennial-scale climatic variability had strong impacts on vegetation (see Fletcher et al. (2010) for a review). In the British Isles, north-west France, the lowlands of the Netherlands, Northern Germany, Denmark and north-west Scandinavia interstadials are characterized by open, treeless vegetation, whereas stadials are often marked by the presence of non-organic deposits indicating a very sparse or absent vegetation (Fletcher et al. (2010) and references therein). In France, the records from lacustrine deposits from La Grande Pile, Les Echets and the Velay maars (Woillard, 1978; de Beaulieu and Reille, 1984, 1992a,b; Reille and de Beaulieu, 1988, 1990) indicate that the last glacial was dominated by steppe-tundra vegetation, with some episodes of open woodland which might correspond to some DO events. The South of Italy (Allen et al., 1999), Alpine regions, the Bay of Biscay and Spain (Fletcher et al., 2010) also show increases in arboreal vegetation during interstadials. In western France, a *Betula-Pinus-deciduous Quercus* forest alternates with steppic plants (Sánchez-Goñi et al., 2008). Several marine cores from the Atlantic or Mediterranean Iberian margins (see Combourieu-Nebout et al., 2002; Sánchez-Goñi et al., 2002; Fletcher and Sánchez-Goñi, 2008; Combourieu-Nebout et al., 2009b) show an alternance of temperate forest during interstadials and steppic vegetation during stadials. The percentage of steppic plants such as *Artemisia* is especially high during stadials associated to a Heinrich event (Combourieu-Nebout et al., 2002; Fletcher and Sánchez-Goñi, 2008; Fletcher et al., 2010). More precisely, southern Iberia is occupied by Mediterranean forest (deciduous and evergreen *Quercus* species) during interstadials and by semi-desert vegetation with *Artemisia*, *Chenopodiaceaea* and *Ephedra* during stadials, and in North-West Iberia deciduous *Quercus* and *Pinus* forest alternates with grass and heathland (Sánchez-Goñi et al., 2008).

To our knowledge, only a few modelling studies have addressed the issue of the vegetation response to abrupt climate changes. Scholze et al. (2003) performed freshwater hosing experiments with the ECHAM3 AOGCM to simulate an idealized analogue of the Younger Dryas and used these climate forcings to run the dynamical global vegetation model (DGVM) LPJ. The strong surface cooling over the Northern Hemisphere leads to a decrease of temperate forests, replaced by boreal forests and C3 grass in northwest Europe and by C3 grass only in Southern Europe.

Köhler et al. (2005) investigated changes in vegetation distribution and land carbon storage at global scale in response to a collapse of the AMOC under different climatic conditions, from the last glacial to the pre-industrial period. They used the LPJ DGVM forced by climatic fields obtained by combining an observation-based climatology, anomalies from freshwater hosing experiments with the ECBILT-CLIO climate model and anomalies from time slice simulations with HadSM3. Their work shows a southward shift of the treeline and reduction of temperate and boreal forests in the North Hemisphere in response to the cooling induced by the collapse of the AMOC, for both pre-industrial and the Last Glacial Maximum (LGM) conditions. The temporal evolution of carbon stocks depends on the initial climatic conditions and initial vegetation distribution. The authors focus essentially on changes in carbon storage and do not give many details on the spatio-temporal response of vegetation distribution. The results obtained by Menviel et al. (2008) with VECODE coupled to LOVECLIM were in qualitative agreement with both studies. Bozbiyik et al. (2011) also investigated the response of the terrestrial carbon cycle to oceanic changes triggered by freshwater pulses in the North Atlantic. Contrary to Köhler et al. (2005) they found large carbon changes in the tropics, with a strong reduction of carbon stocks over South America. Their results suggest that the small CO_2 increase recorded during HE events could be explained by carbon release from the terrestrial biosphere. However, their experiments were performed with a vegetation fixed to its pre-industrial distribution, which can lead to an overestimation of the biosphere contribution to atmospheric CO_2 changes (Köhler et al., 2005).

Kageyama et al. (2005) used the IPSL GCM and the ORCHIDEE DGVM to investigate the impact of Heinrich event 1 (H1) on the climate and vegetation of the western Mediterranean Sea. The climate of H1 was simulated by lowering the SSTs by up to 4 °C over the North Atlantic compared to the control simulation for the Last Glacial Maximum (LGM). The vegetation simulated by ORCHIDEE for H1 presented a strong reduction of tree cover over France and a regression of grass both over France and over the Iberian Peninsula.

In a previous study, Woillez et al. (2011) investigated the relative impact of climate and CO_2 on the vegetation simulated by the ORCHIDEE DGVM at the LGM. The results show that low CO_2 has a strong impact on tree cover response to glacial conditions.This impact depends on both the background climate and the type of vegetation. Here we want to investigate (with the same DGVM) the links between glacial vegetation and the AMOC state, with a focus over Western Europe. How does the vegetation respond to AMOC changes? Can the model reproduce the changes inferred from pollen data for HE and DO events? Is the response synchronous with the AMOC?

We start from the glacial state of vegetation simulated by ORCHIDEE in Woillez et al. (2011) and investigate the response of vegetation to climate changes simulated by the IPSL_CM4 AOGCM in response to abrupt changes in the AMOC strength. We focus on the timing of the response of vegetation compared to the timing of the AMOC evolution and analyse the specific response of the different plant functional types (PFTs) simulated in ORCHIDEE, in order to investigate their different sensitivities to the simulated abrupt climate changes. We also analyse the relative impact of temperature and precipitation changes, which has not been investigated in the studies cited above. Distinguishing the impact of temperature and precipitation might help to better constrain the temperature and precipitation changes inferred from pollen records during abrupt changes.

The layout of the paper is as follows: Sect. 2 describes the ORCHIDEE and IPSL models and the design of the different atmospheric and vegetation runs. In Sect. 3 we present the climatic changes simulated by the model in response to changes in the AMOC strength and the response of vegetation at the global scale. We then focus on Western Europe in Sects. 4 (climate) and 5 (vegetation), a region of special interest given the pollen records available for a model-data comparison. In the present study, we define Western Europe as the area between 32° and 60° N and 15° W and 20° E. We discuss our results and conclude in Sect. 6.

2 Material and methods

2.1 The ORCHIDEE dynamic global vegetation model

ORCHIDEE (Krinner et al., 2005) is composed of three coupled submodels: the surface vegetation-atmosphere transfer scheme SECHIBA, a module for phenology and carbon dynamics of the terrestrial biosphere (STOMATE), and a dynamical vegetation model inspired from LPJ (Sitch et al., 2003). The model simulates the distribution of ten different plant functional types (PFTs) and bare soil (for the list of the PFTs and the corresponding acronyms used in this study see Table 1), which can coexist on the same grid cell, as a result of climatic forcings and competitivity between these different PFTs. The spatial resolution in the vegetation model is identical to the spatial resolution in the climate model. The dynamical part simulates competitive processes such as light competition, sapling establishment, or tree mortality. In this study, ORCHIDEE is forced "offline" by the high-frequency outputs (time step = 6 h) from the IPSL_CM4 model. There is no feedback between vegetation and the atmosphere. The model requires the following variables: temperature, precipitation, specific humidity, wind, surface pressure, shortwave and longwave radiative fluxes.

2.2 The climatic forcings computed with the IPSL_CM4 GCM

The IPSL_CM4 AOGCM (Marti et al., 2010) is composed of LMDz.3.3, the atmospheric general circulation model, and ORCA2, the ocean module. The resolution for the atmosphere is $96 \times 72 \times 19$ in longitude $\times$ latitude $\times$ altitude and a regular horizontal grid. The ocean is simulated over an irregular horizontal grid of 182×149 points and 31 depth levels. The coupling is performed by the OASIS coupler. LMDz includes the surface vegetation model ORCHIDEE (Krinner et al., 2005), sea ice is dynamically simulated by the Louvain-La-Neuve sea Ice Model (LIM2) but glacial ice sheets are fixed. Land, land-ice, ocean and sea ice can coexist on the same grid cell of LMDz.

Four different glacial climatic simulations are performed. The LGM control run (ON_ctrl) is the IPSL PMIP2 LGM run (see LGMb in Kageyama et al., 2009 for details; Braconnot et al., 2007 and http://pmip2.lsce.ipsl.fr for the PMIP2 project). The glacial boundary conditions follow the PMIP2 protocol: ICE-5G reconstruction for the ice sheets (Peltier, 2004); CO_2, CH_4 and N_2O levels set to 185 ppm, 350 ppb and 200 ppb respectively (Monnin et al., 2001; Dällenbach et al., 2000; Flückiger et al., 1999), orbital parameters for 21 ky BP (Berger, 1978). Vegetation is fixed to its present-day distribution on the ice-free areas, including agriculture, since interactive dynamic vegetation is unavailable in this version of IPSL_CM4.

In the ONtoOFF_grad simulation, an additional freshwater flux of 0.1 Sv is imposed instantaneously in the North Atlantic at year 150 of ON_ctrl (see LGMc in Kageyama et al., 2009). The freshwater flux is stopped at year 550. Simulation OFFtoON_grad (resp. OFFtoON_fast) starts at year 550 of ONtoOFF_grad with a negative freshwater flux of -0.1 Sv (resp. -0.5 Sv) imposed in the North Atlantic.

Table 1. Plant functional types (PFT) in ORCHIDEE and acronyms used in this study.

PFT	acronym
Bare soil	Bare soil
Tropical broadleaf evergreen trees	TrBE
Tropical broadleaf raingreen trees	TrBR
Temperate needleleaf evergreen trees	TempNE
Temperate broadleaf evergreen trees	TempBE
Temperate broadleaf summergreen trees	TempBS
Boreal needleleaf evergreen trees	BoNE
Boreal broadleaf summergreen trees	BoBS
Boreal needleleaf summergreen trees	BoNS
C3 grass	C3 grass
C4 grass	C4 grass

The freshwater discharge performed in ONtoOFF_grad leads to a gradual collapse of the AMOC, mimicking the effect of a Heinrich event. The NADW (North Atlantic Deep Water) export at 30° S drops from about 13 Sv in ON_ctrl to 0 Sv within 250 yr of simulation (Fig. 1a). Once the freshwater flux is stopped, the AMOC does not recover and remains in an "off" state. This stability of the collapsed state is not a common behaviour in AOGCMs. In most of them a spontaneous recovery of the AMOC occurs once the freshwater flux is stopped (e.g. Manabe and Stouffer, 1995; Hu et al., 2008; Otto-Bliesner and Brady, 2010).

A gradual recovery occurs in OFFtoON_grad as soon as the negative freshwater flux is imposed. The NADW export reaches the initial state after 250 yr, and stabilizes at 17 Sv about 100 yr later. In OFFtoON_fast, the −0.5 Sv imposed in the North Atlantic leads to a quasi instantaneous recovery of the AMOC, which is back to initial state within about 70 yr. At the end of the simulation, the NADW export is higher than 30 Sv and equilibrium has not been reached (Fig. 1a). This last simulation was designed to mimic the effect of the abrupt warming phase of a DO event. We further describe the climate changes in these runs in Sect. 3.

2.3 Experimental design of the ORCHIDEE off-line runs

Our aim is to simulate the response of the glacial vegetation to abrupt AMOC changes and to investigate whether the vegetation evolution is synchronous with the AMOC, for both a collapse and a recovery at different rates. Therefore, we use the climatic forcings from ON_ctrl, ONtoOFF_grad, OFFtoON_grad and OFFtoON_fast to design different scenarios of AMOC changes and perform six simulations with ORCHIDEE off-line:

– ON_ctrl (1000 yr): the LGM control simulation, forced with 1000 yr of the IPSL simulation ON_ctrl. The simulation starts at the end of a spinup phase designed as follows: ORCHIDEE is run during 500 yr with the ON_ctrl LGM climate, starting from bare ground. Then the soil carbon submodel is run alone for 10 000 yr, to equilibrate the carbon stocks. Finally the whole model is run for another 50 yr (simulation described in Woillez et al., 2011).

– ONtoOFF_grad (800 yr): this simulation starts from the equilibrium state of ON_ctrl and we test the impact of the gradual collapse of the AMOC on vegetation by forcing ORCHIDEE with the climatic forcings from the IPSL simulation ONtoOFF_grad.

– ONtoOFF_inst (400 yr): this simulation starts from the equilibrium state of ON_ctrl and tests the impact of an instantaneous collapse of the AMOC. We impose directly the climate from the last 400 yr of the IPSL simulation ONtoOFF_grad.

– OFFtoON_grad (430 yr): the run starts at year 578 of ONtoOFF_grad and we force the model with the climate from the IPSL simulation OFFtoON_grad, with a gradual recovery of the AMOC.

– OFFtoON_fast (150 yr): the run starts at year 578 of ONtoOFF_grad and we force the model with the climate from the IPSL simulation OFFtoON_fast and a very fast recovery of the AMOC.

– OFFtoON_inst (230 yr): the run starts at year 578 of ONtoOFF_grad and we force the model with the climate from the IPSL simulation ON_ctrl, which corresponds to an instantaneous recovery of the AMOC, but to a value lower than the final value of OFFtoON_grad and OFFtoON_fast (Fig. 1a).

Two additional simulations, starting from the equilibrium state of ON_ctrl, are performed to test the relative impact of temperature and precipitation changes between ON_ctrl and ONtoOFF_grad

– ONtoOFF_precip (428 yr): same climatic forcings as for ON_ctrl except for precipitation, taken from the first 428 yr of ONtoOFF_grad.

– ONtoOFF_temp (428 yr): same climatic forcings as ON_ctrl except for temperature, taken from the first 428 yr of ONtoOFF_grad.

These runs are crude tests, since we do not take into account the fact that climatic variables are not fully independent from one another, but they can nonetheless allow us to test which of these two parameters have the strongest impact on vegetation. We do not test the relative impact of changes in shortwave radiations, wind and specific humidity.

All these ORCHIDEE runs are performed with $pCO_2 = 185$ ppm.

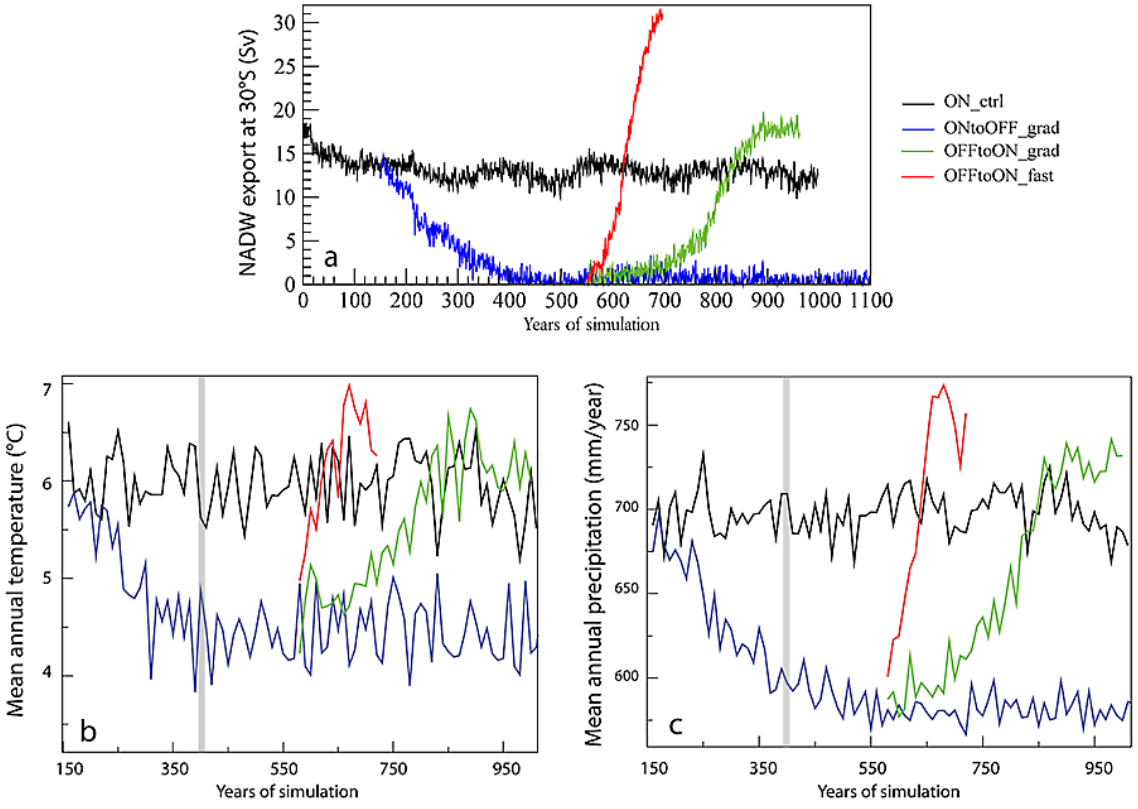

Fig. 1. (a) Temporal evolution of the NADW export at 30° S, in Sv. **(b)** Evolution of the mean annual temperature (°C) and **(c)** the mean annual precipitation over Western Europe (lat = 32/60°, lon = −15/20°) for ON_ctrl, ONtoOFF_grad, OFFtoON_grad and OFFtoON_fast.The curves correspond to values averaged only over the land points and for successive periods of 10 yr of the simulations. The vertical grey bars indicate when the AMOC is fully collapsed in ONtoOFF_grad.

3 Global response of climate and vegetation to AMOC changes

3.1 Climate

The climatic response concomitant with the AMOC collapse has already been described in detail in Kageyama et al. (2009) (comparison between LGMb (= ON_ctrl) and LGMc (= ONtoOFF_grad)). We briefly recall here the main features of the response in the mean annual temperature and annual precipitation. The collapse of the AMOC in ONtoOFF_grad leads to a typical bipolar see-saw, with cooling of the Northern Hemisphere and warming of the Southern Hemisphere (Fig. 2a), as simulated with other models (e.g. Claussen et al., 2003; Kageyama et al., 2010) and in broad agreement with data for stadials (see the review by Voelker, 2002). The strongest temperature anomalies in ONtoOFF_grad compared to ON_ctrl are found over the Atlantic ocean. The mean annual surface air temperature at the end of ONtoOFF_grad compared to ON_ctrl is decreased by more than 5 °C South of Iceland, and by about 4 °C in the mid-latitude North Atlantic. The South Atlantic is warmer by 3–4 °C. The cooling over Eurasia is limited to −1 °/−2 °C and the Pacific side of North America even experiences a warming of about 1 °C (Fig. 2a). The precipitation response (Fig. 2b) is characterized by a strong drying over the North Atlantic and Western Europe and a southward shift of the inter-tropical convergence zone (ITCZ) over the Atlantic basin and adjacent continents, leading to a decrease of precipitation over the Sahel zone (in agreement with data, see Tjallingii et al., 2008) and the north of South America and to an increase over eastern Brazil.

At the end of OFFtoON_grad, the higher AMOC strength (18 Sv, see Fig. 1a) compared to its mean strength in ON_ctrl (about 13 Sv) leads to the opposite response, with a slight northward shift of the ITCZ, leading to a decrease in precipitation of about $-100\,\mathrm{mm\,yr^{-1}}$ over Brazil and an increase in temperature of about 3 °C in the North Atlantic (Fig. 2c, d). The warming over the adjacent continents is limited to about 1 °C over North America and less than 1 °C over the Iberian peninsula. The temperature changes over the rest of Western Europe are not statistically significant and precipitation changes are small and restricted to a few grid cells.

This pattern is enhanced at the end of OFFtoON_fast, for which the AMOC strength reaches 30 Sv (Fig. 1a). The decrease in precipitation is about $-525\,\mathrm{mm\,yr^{-1}}$ over Brazil

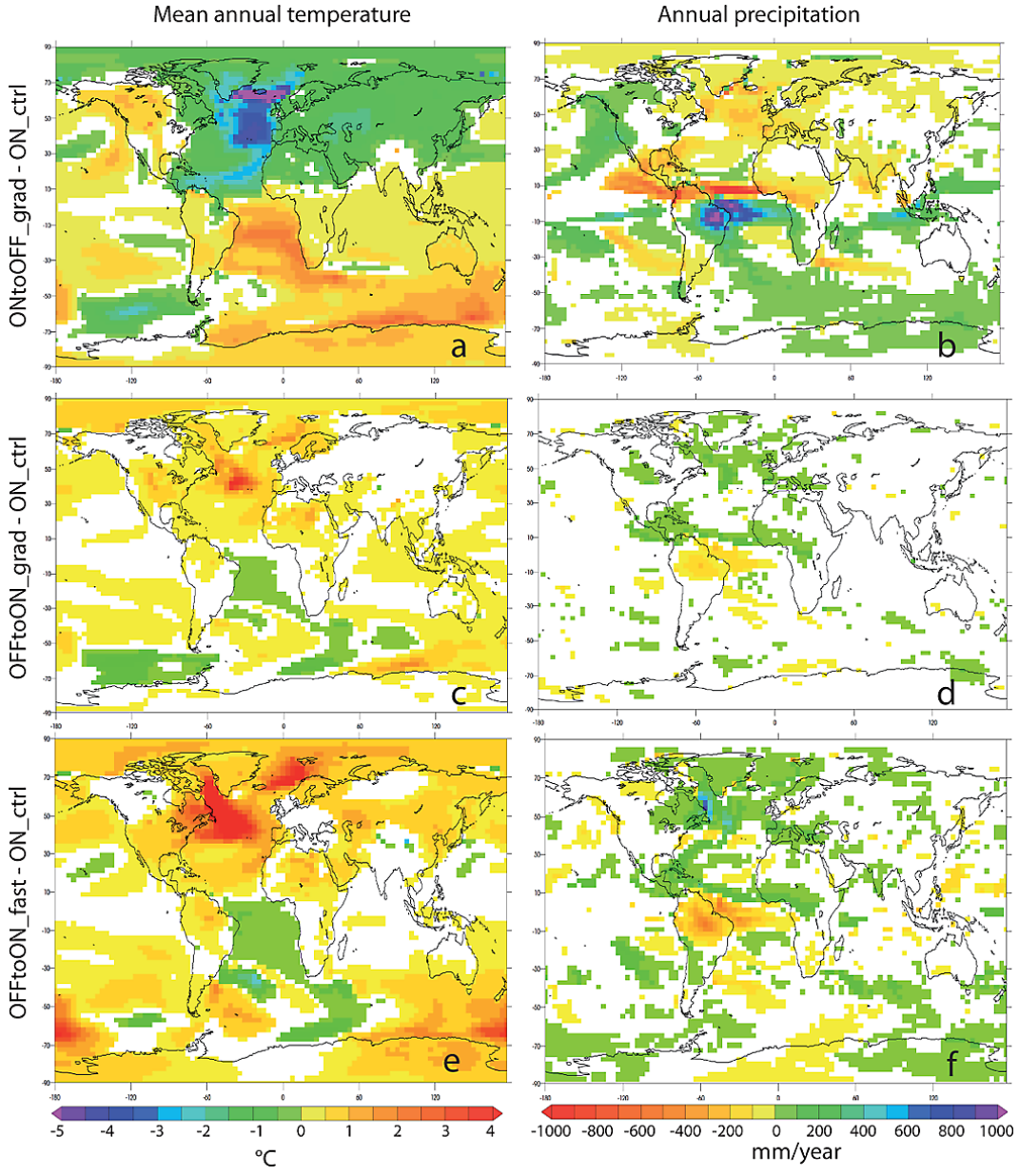

Fig. 2. L.h.s.: difference in mean annual surface temperature (°C). R.h.s.: difference in annual precipitation (mm yr^{-1}). Top: ONtoOFF_grad–ON_ctrl; middle: OFFtoON_grad–ON_ctrl; bottom: OFFtoON_fast–ON_ctrl. White areas are regions were differences are not significant at the 95 % level. ON_ctrl: average over years 201–250; ONtoOFF_grad: average over years 401–450; OFFtoON_grad: average over the last 30 yr of the run; OFFtoON_fast: average over the last 20 yr of the run.

and a strong warming occurs in the North Atlantic (Fig. 2e, f). The increase in the surface air temperature is about 6 °C at 50° N, up to 10 °C in the Labrador Sea and about 3 °C at 70° N. The temperature increase in the Labrador Sea is associated to an increase in precipitation of about 700 mm yr^{-1}. This pattern is due to changes in the sea ice extent. The see-saw effect is however less strong than in ONtoOFF_grad and the South Hemisphere does not exhibit a strong cooling. The temperature decrease in the South Atlantic is less than 1 °C and we even notice a warming in the region of the Weddell Sea. However, the simulation is not at equilibrium and this pattern could be a transient response.

As for ONtoOFF_grad, the temperature anomalies simulated over the North Atlantic at the end of ONtoOFF_fast do not propagate far inland over Western Europe. Changes in precipitation are also limited to the Mediterranean region (Fig. 2e, f). This limited inland propagation of temperature anomalies is consistent with the development of an

anticyclonic anomaly over the North Atlantic which brings colder air from the high latitudes over Europe. The opposite phenomenon occurs when the AMOC collapses: a cyclonic anomaly develops over the North Atlantic and brings warmer air from the south over Europe, limiting the cooling over this region (Kageyama et al., 2009).

The global temperature pattern in OFFtoON_fast is in broad agreement with data for interstadials (Voelker, 2002), but precipitation changes seem to be underestimated (Voelker, 2002). The detailed analysis of oceanic and atmospheric changes at the end of OFFtoON_grad and OFFtoON_fast compared to ON_ctrl is beyond the scope of the paper and is left for another study.

3.2 Vegetation

The performance of ORCHIDEE in simulating the glacial vegetation has been previously described by Woillez et al. (2011). Figure 3a presents the total forest, grass and bare soil fractions simulated in ON_ctrl (corresponding to simulation LGMG in Woillez et al., 2011). ORCHIDEE correctly reproduces the main features of glacial vegetation, with high grass fractions over Siberia, in agreement with pollen data, indicating the dominance of steppic vegetation (Prentice et al., 2000), and the reduction of tropical forests compared to present-day, particularly over the Amazon Basin, where tree fractions are lower than 30 %. The main biases are an important overestimation of the bare soil fractions over India, southern Africa and South America, as well as an overestimation of the remaining tree fractions over Western Europe, eastern Eurasia and the Atlantic coast of North America.

The vegetation simulated at the end of ONtoOFF_grad is presented in Fig. 3b (absolute vegetation fractions) and Fig. 3c (anomalies). The main differences between ONtoOFF_grad and ON_ctrl are an increase of forests over East Brazil, a decrease over central America and equatorial Africa, a reduction of forests over Western Europe, replaced by grasses, and a decrease of grasses over the Beringia region. The increase of forest over South America at the expense of the bare soil fraction is due to the strong increase of precipitation over this area in response to the displacement of the ITCZ (Fig. 2b). The opposite trend is simulated at the end of OFFtoON_grad and OFFtoON_fast compared to ON_ctrl: the decrease in precipitation leads to a decrease in trees fractions (Fig. 4a, b). This result is in qualitative agreement with pollen data for South America (Hessler et al., 2010). The records with sufficiently high resolution to investigate the response of vegetation to millennial-scale variability in this region are rather sparse, however a few sites from the northern and southern present-day limit of the ITCZ support the hypothesis of a southward migration of the ITCZ during HE events: in the Cariaco Basin, interstadials are characterized by an expansion of forests and stadials by the dominance of savannah, whereas records from northeastern Brazil show the opposite trend, with increasing forest taxa during some HE events, indicating wetter conditions (Hessler et al., 2010). Both Köhler et al. (2005) and Menviel et al. (2008) simulate only small changes in the vegetation of South America in response to an AMOC collapse, due to limited changes in the position of the ITCZ. Our results are in qualitative agreement with the findings of Bozbiyik et al. (2011), showing a strong decrease in precipitation and consequently in terrestrial carbon over the north of South America. However, they do not simulate a vegetation increase over Brazil. These differences in our results and previous studies highlights the interest of further investigation in the tropical response to AMOC changes, to assess quantitatively the contribution of tropical vegetation to changes in the carbon cycle during Heinrich events.

The vegetation response over Europe, with regression of forest and development of C3 grass when the AMOC collapse and opposite response when the AMOC recovers, is investigated in detail in the following sections.

4 Climatic response to changes of the AMOC over Western Europe

Before investigating the European vegetation response to the climatic changes related to the AMOC collapse and resumption, we present this climatic response in more details in the following sections. We first compare the temperature and precipitation simulated by IPSL_CM4 in ON_ctrl to the reconstructions from Wu et al. (2007) and then present the climatic changes in ONtoOFF_grad, OFFtoON_grad and OFFtoON_inst.

4.1 Model-data comparison for the LGM control run

4.1.1 Temperature

We compare the mean temperature of the warmest month (MTWA) and the mean temperature of the coldest month (MTCO) simulated by IPSL_CM4 in ON_ctrl for Western Europe to the reconstructions by Wu et al. (2007), for three latitude bands (see Fig. 5). Their method is based on inverse modelling using the BIOME4 vegetation model, thus taking into account the effect of low glacial atmospheric CO_2 on vegetation. The IPSL model correctly simulates the MTWA changes (Fig. 5b), but the amplitude of the MTCO changes are systematically underestimated by several degrees compared to the median reconstructions (Fig. 5a). The model is too warm by more than 10 °C in the western band (sector A) below 45° N, by about 8 to 10 °C in the central band (sector B), between 40 and 50° N and by about 5 °C in the eastern band (sector C) around 42° N. However the model results lie within the uncertainty range of the reconstructions. The underestimation of the coldest temperature in Western Europe is a common bias in GCMs and results from IPSL_CM4 are

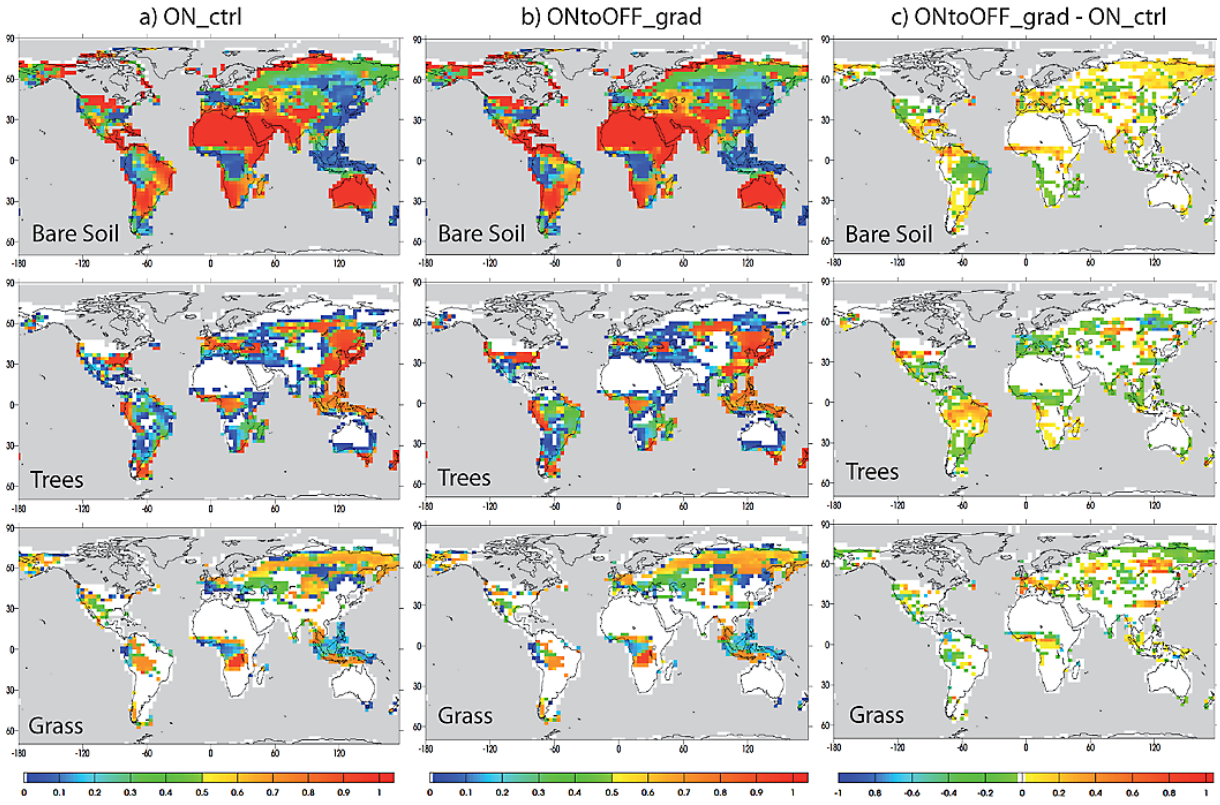

Fig. 3. Fractions of bare soil, trees and grass (between 0 and 1) simulated by ORCHIDEE in **(a)** ON_ctrl (average over 500 yr of run), **(b)** ONtoOFF_grad (average over the last 200 yr of run) and **(c)** differences between ONtoOFF_grad and ON_ctrl.

similar to those from the other models of the PMIP2 data base (in grey in Fig. 5).

4.1.2 Precipitation

Model-data comparison for anomalies in annual precipitation in ON_ctrl compared to the reconstructions of Wu et al. (2007) are presented in Fig. 6. The model simulates annual precipitations similar or slightly above the present-day values for the three longitude bands considered. These values are within the uncertainty range of the reconstructions by Wu et al. (2007). However, precipitation over the Iberian peninsula are probably overestimated since the simulated values exceed the mean reconstruction by about 500 mm yr^{-1} (Fig. 6, sector A, 43° N). Temperatures simulated for this region are also overestimated by 10 °C (MTCO, see Fig. 5a) compared to Wu et al. (2007) reconstructions, suggesting an overestimation of the advection of relatively warm and humid air from the ocean. This is consistent with a strong AMOC, which is more active than estimated from reconstructions (McManus et al., 2004; Piotrowski et al., 2005).

4.2 Response to the AMOC collapse and recovery

4.2.1 Temperature

The evolution of the mean annual temperature inland over Western Europe in ONtoOFF_grad follows the gradual collapse of the AMOC, with a decrease from about 6 °C (interannual standard deviation: 0.75 °C) in ON_ctrl to 4.3 °C (interannual standard deviation: 0.76 °C) over the last 400 yr of ONtoOFF_grad (Fig. 1b). The comparison of Fig. 1a and Fig. 1b shows there is no lag between the temperature evolution and the AMOC strength. For both variables, equilibrium is reached at the same time.

The anomaly of temperature observed in the North Atlantic (−4 °C in ON_ctrl compared to ONtoOFF_grad at equilibrium) does not propagate far inland. Fig. 7 shows the differences between ONtoOFF_grad at equilibrium and ON_ctrl for the mean annual temperature (MAT, Fig. 7a), the mean temperature of the coldest month (MTCO, Fig. 7b) and the mean temperature of the warmest month (MTWA, Fig. 7c). The MAT decreases by about −2 °C on the Atlantic side, and −1.5 to −2 °C inland in France and Iberia. The cooling in the western part of the Mediterranean and in Germany is −1 to −2.5 °C , and less than 1 °C in Italy. Changes in the MTCO range from about −3 °C on the

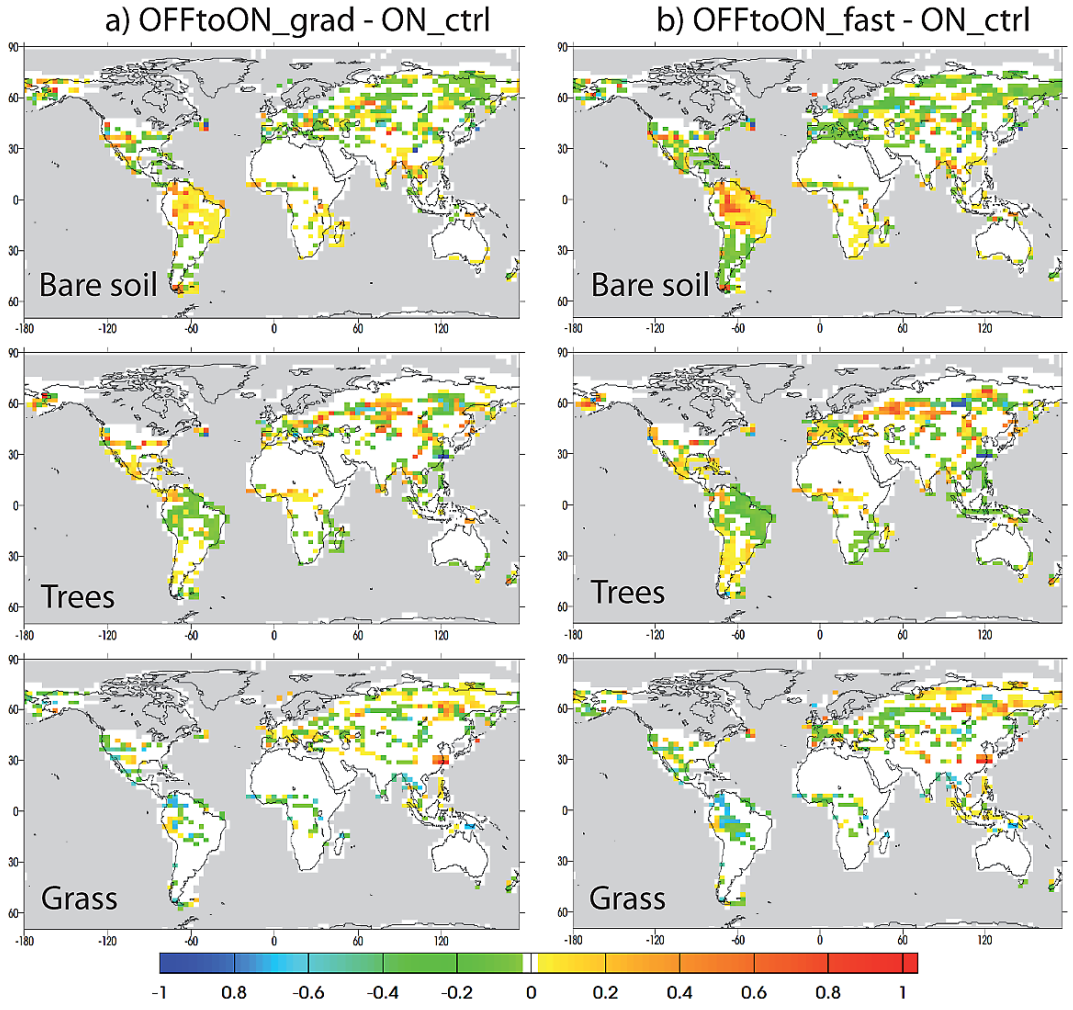

Fig. 4. Differences in the fractions of bare soil, trees and grass simulated by ORCHIDEE at the end of **(a)** OFFtoON_grad and **(b)** OFFtoON_fast compared to ON_ctrl. OFFtoON_grad: average over the last 30 yr of the run. OFFtoON_fast: average over the last 20 yr of the run. ON_ctrl: average over 500 yr of run.

Iberian Atlantic margin to only −1.5 to −1 °C in central France. MTCO anomalies in eastern France, Germany and Italy are not statistically significant. The decrease in MTWA is always smaller in amplitude than −1.5 °C, except for the north and west of France, south-west Iberia and the North Atlantic coast of Iberia (−2 to −2.5 °C). The cooling associated to the AMOC collapse is stronger than the cooling simulated by Kageyama et al. (2005) with the same atmospheric model by prescribing SST anomalies of −4 °C in the North Atlantic to mimic the Heinrich event 1. In their study, MTCO was reduced by less than 2 °C on the Atlantic side over Iberia, and less than 1 °C in central Iberia and the French Atlantic coast. However, the cooling in the MTCO simulated in this study at the end of ONtoOFF_grad is still too small when compared to palynological reconstructions based on the modern analogue technique (Guiot, 1990). For H1 around the Alboran Sea for instance (ODP site 976), the reconstructed anomalies compared to the LGM are between −5 to −15 °C (Kageyama et al., 2005; Combourieu-Nebout et al., 2009b). The simulated decrease in the MAT is closer to reconstructions of a decrease of about −2.6 °C (N. Combourieu-Nebout, personal communication, 2012). However, it is known that the reconstructions based on the modern analogue technique have a tendency to underestimate the MTCO (Combourieu-Nebout et al., 2009b; Wu et al., 2007). Moreover, the lack of modern analogue of the LGM vegetation adds uncertainties to the method, which in addition does not take the effect of low CO_2 on vegetation into account.

The underestimation of the cooling amplitude can be partly attributed to the lack of resolution in the model, since the Mediterranean Sea is crudely represented, which limits the impact inland of the SST cooling on the Mediterranean side. The limited cooling is also explained by the development of a cyclonic anomaly in ONtoOFF_grad bringing

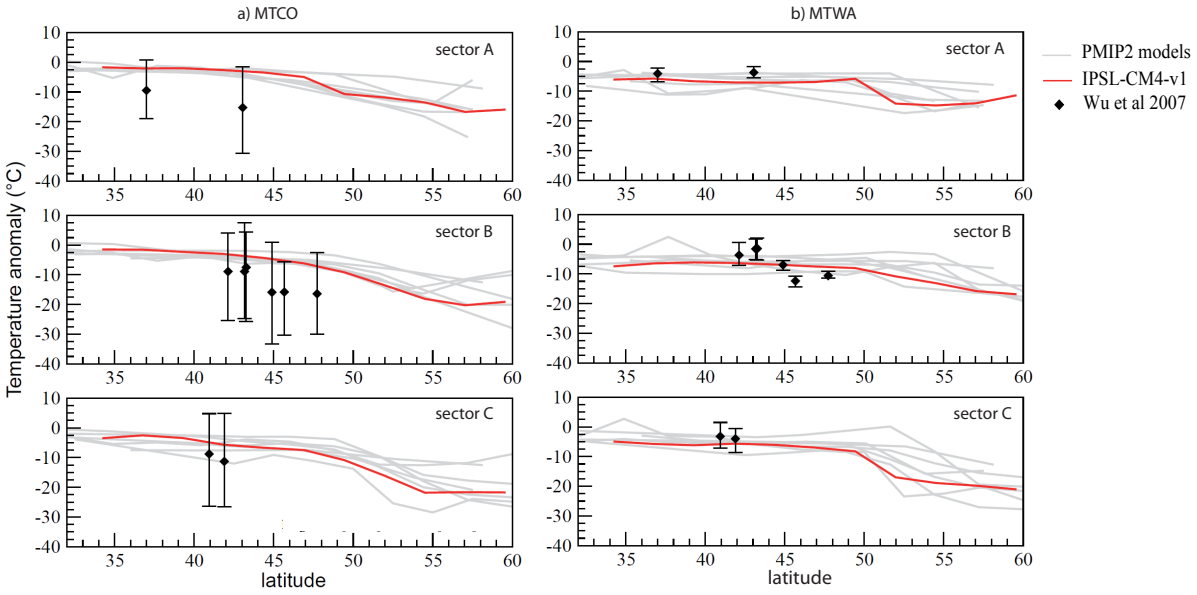

Fig. 5. Difference in **(a)** the mean temperature of the coldest month (MTCO) and **(b)** mean temperature of the warmest month (MTWA) between the LGM and present-day simulated by IPSL_CM4 (red) and other GCMs from the PMIP2 project (grey), for 3 longitude bands over Western Europe, between 32° and 60° N. The limits of the three sectors are plotted in Fig. 8. Sector A: lon = −15/-2°, Sector B: lon = −2/10°, Sector C: lon = 10/20°. Black diamonds are MTWA and MTCO values reconstructed by Wu et al. (2007) with the associated uncertainty range.

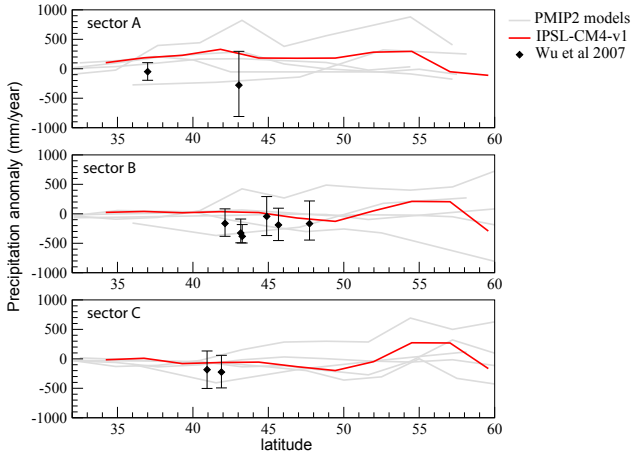

Fig. 6. Difference in annual precipitation (mm yr^{-1}) between the LGM and present-day simulated by IPSL_CM4 (red) and other GCM from the PMIP2 project (grey), for 3 longitude bands over Western Europe, between 32° and 60° N. The limits of the three sectors are plotted in Fig. 8. Sector A: lon = −15/−2°, Sector B: lon = −2/10°, Sector C: lon = 10/20°. Black diamonds are precipitation values reconstructed by Wu et al. (2007) with the associated uncertainty range.

relatively warm air from the south-west to Western Europe, as mentioned in Sect. 3 (see also Kageyama et al., 2009).

When the AMOC gradually recovers in OFFtoON_grad the mean annuel temperature rises again and stabilises slightly above the value of ON_ctrl. Similarly, in OFFtoON_fast the mean annual temperature follows the AMOC evolution, the temperature abruptly rising by about 2.5 °C (Fig. 1b). Thus the impact of AMOC changes on European temperature is clearly unlinear since an AMOC collapse from 15 to 0 Sv leads to a temperature decrease of about 2 °C, whereas an increase from 15 to 30 Sv leads to a rise in temperature of about 1 °C.

4.2.2 Precipitation

When the AMOC collapses, we observe a gradual decrease in mean annual precipitation from 700 ± 35 mm yr^{-1} in ON_ctrl to 580 ± 32 mm yr^{-1} in ONtoOFF_grad over the last 400 yr of simulation (see Fig. 1c). The decrease in precipitation follows the decrease in the AMOC strength.

At equilibrium, the precipitation decrease in ONtoOFF_grad compared to ON_ctrl is between −110 and −200 mm yr^{-1} over France, around −200 mm yr^{-1} in northern Iberia and −100/−150 mm yr^{-1} in southern Iberia. The strongest decrease occurs in NW Iberia, with −337 mm yr^{-1} (Fig. 8).

Expressed in percentages, these changes correspond to a decrease of −10/−20 % over France and −25/−30 % in Iberia. These values are of the same order than the ones in Kageyama et al. (2005) and are in qualitative agreement with palynological reconstructions indicating a drier climate during HE events. However, the simulated decrease in precipitation is underestimated, palynological reconstructions

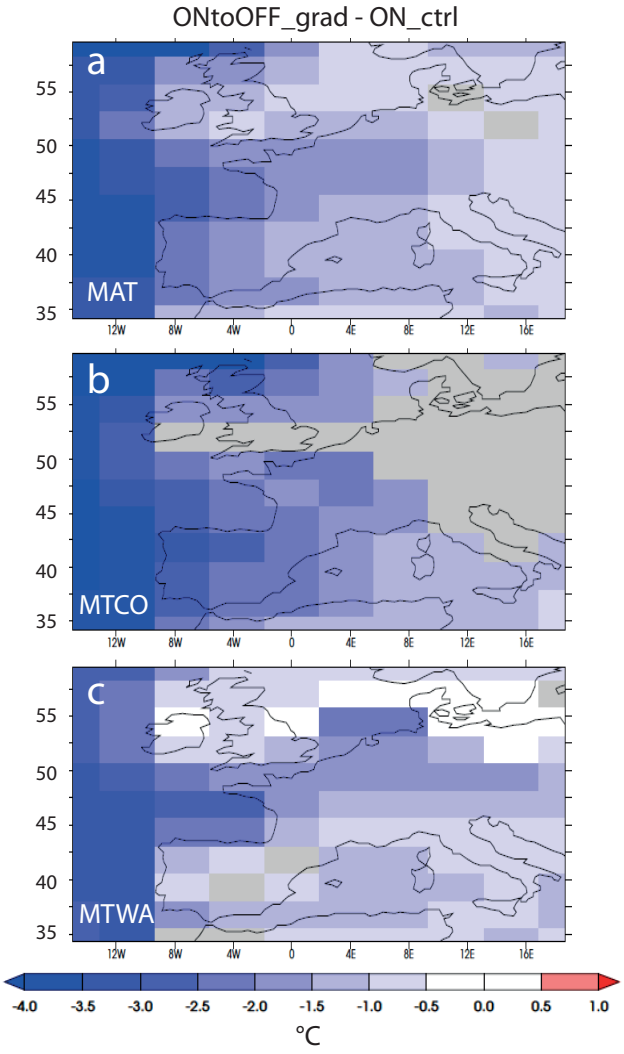

Fig. 7. Difference between ON_ctrl and the end of ONtoOFF_grad for **(a)** the mean annual temperature (MAT), **(b)** mean temperature of the coldest month (MTCO) and **(c)** mean temperature of the warmest month (MTWA) (°C). Grey areas are points where the difference is not significant at the 95 % level.

indicating a decrease of up to $-214\,\mathrm{mm\,yr^{-1}}$ between H1 and the LGM in western Mediterranean for instance (Alboran ODP site 976, N. Combourieu Nebout and I. Dormoy, personal communication, 2012). Our results are closer to the amplitude of change reconstructed between a stadial without Heinrich event and an interstadial for the Alboran Sea by Sánchez-Goñi et al. (2002).

When the AMOC recovers, in OFFtoON_grad and OFFtoON_fast, the mean annual precipitation rises again and reaches about $730\,\mathrm{mm\,yr^{-1}}$ at the end of OFFtoON_grad and more than $750\,\mathrm{mm\,yr^{-1}}$ at the end of OFFtoON_fast, i.e. an increase of only 30 and $50\,\mathrm{mm\,yr^{-1}}$, respectively, compared to ON_ctrl (Fig. 1c). The impact of the very high circulation rate of the AMOC at the end of OFFtoON_fast compared

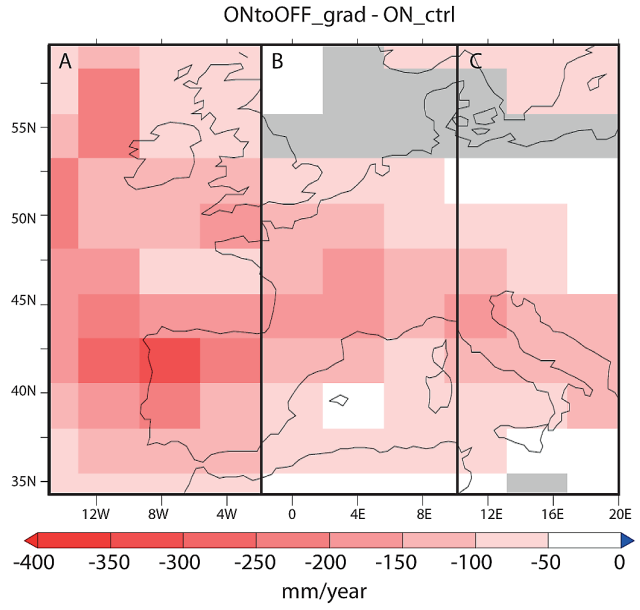

Fig. 8. Difference in annual precipitation (mm/year) between ON_ctrl (average over 500 yr) and the end of ONtoOFF_grad (average over the last 200 yr of the run). Grey areas are points where the difference is not significant at the 95 % level.

to ON_ctrl on European precipitation is thus much smaller than the impact when the AMOC collapses (ONtoON_grad). Thus, similarly as for temperatures, the impact of AMOC on precipitation for changes around the value of ON_ctrl is not linear.

5 Response of the European glacial vegetation to abrupt AMOC changes

5.1 Glacial vegetation in the control run

5.1.1 Model-data comparison for the LGM control run

The glacial vegetation simulated over Western Europe by ORCHIDEE in ON_ctrl is characterized by high tree fractions (Fig. 9). France is covered by needleleaf forests (60–70 %), with TempNE on the Atlantic side and BoNE more inland. East of 6° E and north of 48° N, forests are replaced by C3 grass. The Iberian peninsula is essentially covered by BoBS (40 % on the Atlantic side and more than 70 % near the Pyrenees). This PFT is also present in the region of the Adriatic Sea (60–70 %). South of 38° N, the Mediterranean region is semi-desertic, with only small fractions of TempBS (10–15 %), and TempBE in southern Iberia. Other PFTs are not present. An additional LGM simulation performed with a water-saturated soil (to prevent water stress on vegetation) shows that the tree PFTs are limited eastward and northward by the cold temperatures, and southward by the lack of water (Woillez, 2012).

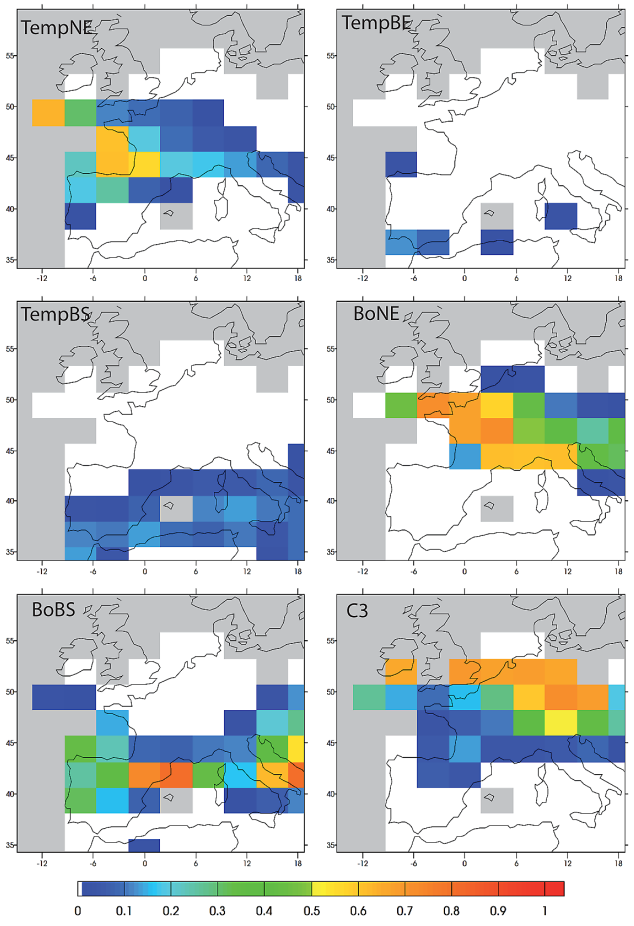

Fig. 9. Fractions of grid cells occupied by the different PFTs (annual maximum, between 0 and 1) simulated by ORCHIDEE in ON_ctrl over Western Europe. The values are averages over the last 500 yr of the run. PFT acronyms: see Table 1. Grey areas are occupied by ocean or ice sheets.

When compared to pollen reconstructions, the vegetation simulated by ORCHIDEE for the LGM appears to be closer to an interstadial than to a LGM vegetation. Indeed, pollen data for the LGM indicate the dominance of steppe-tundra vegetation over France (Fletcher et al., 2010), a herbaceous-dominant environment with Pinus and scattered pockets of deciduous trees in Iberia (Roucoux et al., 2005; Naughton et al., 2007), and shrubby vegetation with high values for semi-desert taxa in southern Iberia (Fletcher and Sánchez-Goñi, 2008), associated with *Cedar* forest at high altitude (Combourieu-Nebout et al., 2009b). Thus our results for the Mediterranean, showing only small tree fractions, are in qualitative agreement with data, despite the lack of grasses, but further north forests are clearly overestimated. ORCHIDEE simulates a clear N / S gradient in vegetation, with semi-desertic vegetation in southern Iberia, BoBS forest in northern Iberia then gradually replaced by TempNE and BoNE over France and finally C3 grass. This gradient can be compared to the gradient observed in pollen data by Sánchez-Goñi et al. (2008) for interstadials. They show a progressive transition from deciduous Mediterranean and temperate forests in Iberia to boreal forests with more *Betula* and *Pinus* over France. Forest fractions in ON_ctrl are overestimated even for an interstadial, but ORCHIDEE qualitatively reproduces the transition between broadleaf and needleleaf forests. The main discrepancy with pollen data for an interstadial is the high fractions of BoBS over Iberia, which can be at least partly attributed to the systematic overestimation of this PFT in ORCHIDEE (see Woillez et al., 2011). For the Adriatic region, LGM records indicate landscapes occupied by semi-desert taxa at low elevation and the presence of conifers at high altitudes, while deciduous forests were only poorly represented (Combourieu-Nebout et al., 1998). Our results are only in partial agreement with this reconstruction. ORCHIDEE reproduces correctly the absence of temperate PFTs and presence of BoNE (40 %), but grasses are clearly underestimated and BoBS overestimated (40 to 70 %), a general bias of the ORCHIDEE model (Woillez et al., 2011).

However, model-data comparison for vegetation can only remain qualitative, due to the coarse resolution of the vegetation model, related to the coarse resolution of the climate model forcings. Particularly, the pollen record at one site can reflect the surrounding vegetation at different elevations, and the model does not allow us to consider vegetation changes with altitude within a grid box.

The overestimation of forest in Western Europe for the LGM is a common bias in vegetation simulations (see Köhler et al., 2005; Kageyama et al., 2005; Menviel et al., 2008). For the present study, this excess of forest can be partly attributed to the bias in the climatic forcings, too warm and wet compared to reconstructions (see Sect. 4.1).

5.1.2 Variability of glacial vegetation over Western Europe

Figure 10a shows the temporal evolution of the surface covered by each PFT during ON_ctrl. The area occupied by TempNE and TempBS is stable, at about 270×10^3 and 80×10^3 km^2, respectively. The areas of BoNE and C3 grass are more variable, with values between 570 and 750×10^3 km^2 for BoNE, and between 420 and 700×10^3 km^2 for C3 grass. The PFT showing the highest variability at centennial scale is BoBS, with values ranging from 280 to 720×10^3 km^2. Thus, vegetation over Western Europe appears to be very sensitive to the variability of the LGM climate as simulated by the IPSL model. This sensitivity is linked to the low level of atmospheric CO_2, since for a simulation where a glacial climate but modern CO_2 for photosynthesis is prescribed, the vegetation is rather stable (results not shown). Woillez et al. (2011) showed that the level of atmospheric CO_2 has a strong impact on the response of vegetation to a given climate in ORCHIDEE. In particular, they showed that low CO_2 reduces the area of viability for a

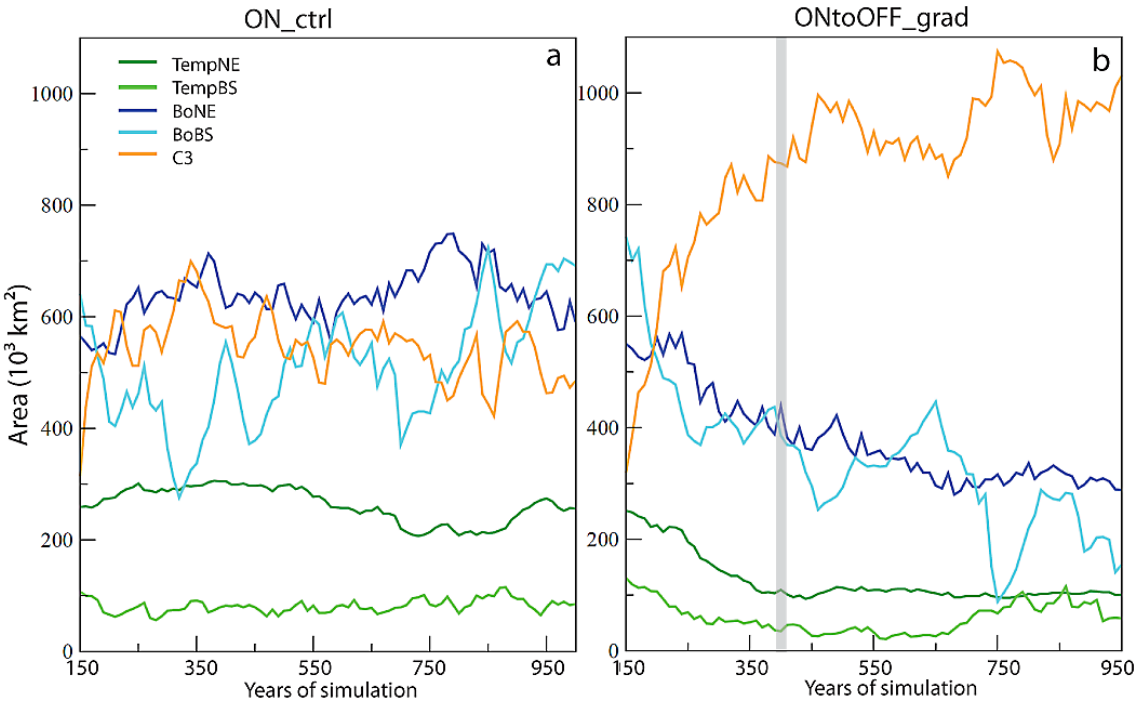

Fig. 10. Temporal evolution of the area occupied by each PFT over Western Europe (lat = 32/60°, lon = −15/20°) in **(a)** ON_ctrl and **(b)** ONtoOFF_grad (10^3 km^2, values are averages over 10 yr of run). The vertical grey bar indicates the full AMOC collapse. PFT acronyms: see Table 1. The area of TempBE remains below 20×10^3 km^2 and this PFT has been omitted on both graphs.

given PFT, and leads to a decrease in productivity, but they did not investigate the response to climatic variability. The high vegetation variability observed in ON_ctrl can be attributed to the increased sensitivity of vegetation to drought or cold temperatures under low CO_2. Therefore, threshold conditions for survival are probably more often crossed than they are under modern CO_2, when the tolerable climatic range is broader.

5.2 Vegetation response to AMOC changes

5.2.1 Collapse of the AMOC

Gradual collapse

Figure 10b gives the temporal evolution of the area occupied by each PFT in ONtoOFF_grad. All PFTs react immediately to the change in climate due to the gradual collapse of the AMOC. However, equilibrium is not reached at the same time for each PFT. The evolution of TempNE and TempBS follows the decrease of the AMOC and the areas of these two PFTs reach their minimum in 250 yr. The slight increase of TempBS over the last 200 yr of the run corresponds to its development over only one grid cell in southwest Iberia and is therefore not really significant. BoNE reach equilibrium after about 500 yr of simulation and their area stabilizes at 300×10^3 km^2 (600×10^3 km^2 in ON_ctrl). The decrease of BoBS starts immediately at the beginning of the AMOC collapse, but given the high variability of this PFT in ON_ctrl, the decrease only gets significant after about 500 yr of simulation, with values around 200×10^3 km^2 (vs generally more than 400×10^3 km^2 in ON_ctrl, cf. Fig. 10a). Boreal forests thus continue to regress during about 200 yr after climatic equilibrium (see Fig. 1b, c for the temporal evolution of the mean annual temperature and precipitation over Europe during ONtoOFF_grad). C3 grasses essentially expand over areas primarily occupied by forests, their temporal evolution is anti-correlated with the one of the tree PFTs. Equilibrium is reached after about 400–500 yr of simulation, around 1000×10^3 km^2 ($500–600 \times 10^3$ km^2 in ON_ctrl).

Figure 11 presents the final vegetation fractions for each PFT at equilibrium in ONtoOFF_grad. Compared to ON_ctrl (Fig. 9), TempNE have nearly totally disappeared from Iberia and subsist only on the French Atlantic coast, with fractions between 40–60 %. TempBS have regressed over all the Mediterranean, and occupy only a few percentages of the grid cells where they are still present. The treeline of the BoNE forest migrates west and southward. Its northern limit regresses by about 3°, and its eastern limit is displaced from about 10–12° E in ON_ctrl to 6° E in ONtoOFF_grad. In northern Italy, BoNE fractions drop from 50–60% to less than 20 %; in Germany the remaining fractions are less than 5 %. High fractions (60 %) only subsist in south-west France, where they replace TempNE. BoBS are also strongly reduced, and almost disappear in Iberia, the small remaining

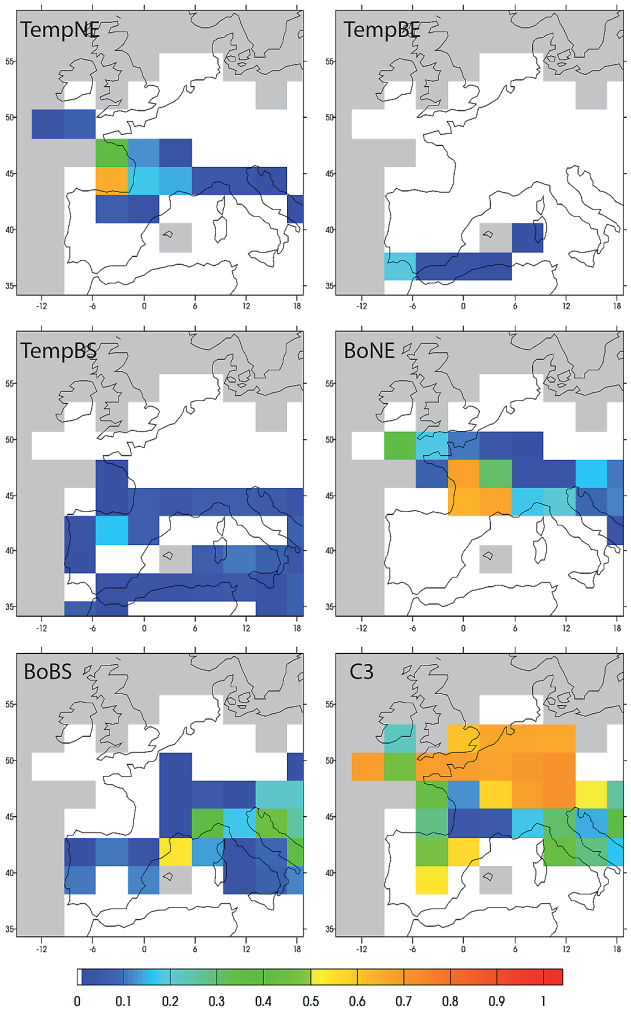

Fig. 11. Vegetation fractions (annual maximum) simulated by ORCHIDEE at the end of ONtoOFF_grad. The values are means over the last 200 yr of the run. PFT acronyms: see Table 1. Grey areas are occupied by ocean or ice sheets.

patches having fractions around 10 % only, but they subsist in the east, with fractions between 20 to 40 %. Correlatively to this general regression of tree PFTs, C3 grass expands in France, Italy and northern Iberia.

The regression of forests and the development of grasses is in qualitative agreement with pollen data (see Sect. 1). However, ORCHIDEE still overestimates forests in south-west France and overestimates the effect of the aridity simulated by IPSL_CM4 over Iberia since the west and south of the peninsula are dominated by bare soil, a bias already present in ON_ctrl.

Our results are also in qualitative agreement with Kageyama et al. (2005). However, the vegetation simulated at initial state in their study is quite different from ours, with smaller tree fractions over France and almost no trees over Iberia, whereas grass fractions are much higher, with about 30 % in central France and 20 % in Iberia. As a result, in their study the "H1" climate leads to forest regression over France only, and also to a decrease in grass fractions both over France and Iberia.

Comparison to an instantaneous collapse

In order to assess the sensitivity of the vegetation to the rate of the AMOC collapse, we now compare the temporal evolution of the total area covered by forest (Fig. 12a) and the area covered by C3 grass (Fig. 12b) in response to a gradual (ONtoOFF_grad) or instantaneous (ONtoOFF_inst) AMOC collapse. How long is the lag between climate and vegetation when the change in climate corresponding to the "off" state of the AMOC is imposed instantaneously?

In ONtoOFF_grad, the forested area gradually decreases from $1600 \times 10^3\,km^2$ to $800 \times 10^3\,km^2$ within 300 yr of simulation, remains stable during 300 yr, then briefly collapses to about $600 \times 10^3\,km^2$ before increasing again at $800 \times 10^3\,km^2$ and finally decreases at $600 \times 10^3\,km^2$ at the end of the run. The high variability of forest cover, already described previously, is thus also present when the AMOC is collapsed and makes it difficult to precisely determine when the vegetation has reached its final state. We can consider that the equilibrium is reached after about 500–600 yr of simulation, i.e. about 200–300 yr after the AMOC full collapse.

When the climate for a collapsed AMOC is imposed instantaneously (ONtoOFF_inst), as could be expected the decrease in forested areas occurs more rapidly. It starts with an abrupt shift to $1250 \times 10^3\,km^2$ during the first 25 yr of simulation, followed by a more gradual decrease and equilibrium is reached after about 200 yr of simulation. Hence an instantaneous climate change corresponding to an AMOC collapse does not immediately kill all the trees. Rather, the gradual regression of forest cover after the instantaneous change of climate appears to be linked to the succession of unfavourable years over a long period.

Thus, in both simulations, a time lag of about 200 yr is observed between the equilibrium state of the AMOC and the equilibrium of forested areas. The evolution of the C3 grass area is different, since the rate of increase is approximately the same in ONtoOFF_grad and ONtoOFF_inst. In both simulations, the total area gradually increases from $350 \times 10^3\,km^2$ to $1000 \times 10^3\,km^2$ within 400 yr. This apparent similar evolution actually hides spatial differences, with a slower spatial expansion of C3 grasses in ONtoOFF_grad, but with higher fractions than in ONtoOFF_inst.

5.2.2 Relative impact of changes in temperature and precipitation during a gradual collapse of the AMOC on forest cover

It is quite interesting that the relatively small changes in temperature and precipitation described in Sect. 4.2 leads to the drastic vegetation changes described in Sect. 5.2.1. As

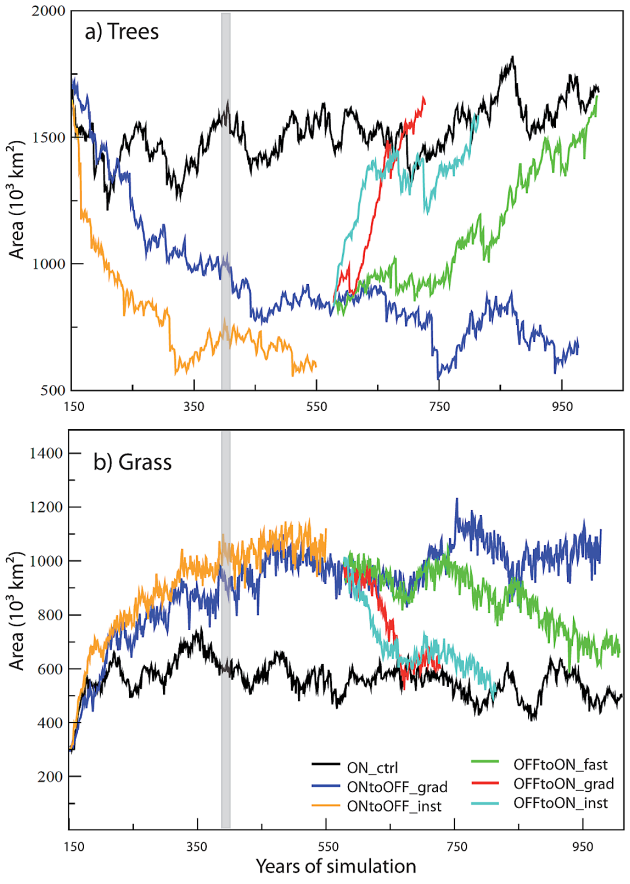

Fig. 12. Area of Western Europe (lat = 32/60°, lon = −15/20°) occupied by **(a)** tree PFTs and **(b)** grass in ON_ctrl (black), ONtoOFF_grad (blue), ONtoOFF_inst (orange), OFFtoON_grad (green), OFFtoON_fast (red), OFFtoON_inst (turquoise). The vertical grey bars indicate when the AMOC is fully collapsed in ONtoOFF_grad.

a first step towards understanding the reasons for these vegetation changes, we investigate the relative impact of temperature and precipitation changes in ONtoOFF_grad on European vegetation. We first compare the total area covered by TempNE, BoNE and BoBS in ON_ctrl, ONtoOFF_temp, ONtoOFF_precip and ONtoOFF_grad (Fig. 13).

For both TempNE and BoNE (Fig. 13a, b), changes in precipitation alone (ONtoOFF_precip) are not sufficient to drive the decrease observed in ONtoOFF_grad. For BoNE, the curves of ON_ctrl and ONtoOFF_precip are even almost exactly the same. On the contrary, when we consider ONtoOFF_temp, TempNE and BoNE areas decrease more or less in the same way as in ONtoOFF_grad. We can conclude that for needleleaf evergreen trees, for which the highest fractions are over France, the area changes when the AMOC collapse are caused by temperature changes and not by precipitation changes.

The area occupied by BoBS (Fig. 13c) in ONtoOFF_precip and ONtoOFF_temp does not really stand out of the variability observed in ON_ctrl. Areas for the last 50 yr of ONtoOFF_precip and ONtoOFF_temp are approximately the same ($400–500 \times 10^3$ km^2), i.e. reduced compared to the area in ON_ctrl ($500–600 \times 10^3$ km^2) over the same period, though still within the variability of ON_ctrl, whereas in ONtoOFF_grad BoBS area is below 400×10^3 km^2. Thus, at European scale both temperature and precipitation play a role in the evolution of this PFT in ONtoOFF_grad. This result can be refined when considering two smaller regions where BoBS are abundant in ON_ctrl: Iberia and the Italian and Adriatic regions. In Italy (Fig. 14b), changes in temperature alone lead to an increase of BoBS area, from 100×10^3 km^2 to $150–200 \times 10^3$ km^2, whereas changes in precipitation alone tend to make the BoBS area decrease. The respective impact of temperature and precipitation changes compensate and in ONtoOFF_grad the area occupied by BoBS is not different from ON_ctrl. The results are different for Iberia (Fig. 14a): the evolution of the BoBS area in ONtoOFF_precip is similar to ON_ctrl, and the evolution in ONtoOFF_temp similar to ONtoOFF_grad, which shows that temperature change is the main driver of BoBS decrease over the peninsula in ONtoOFF_grad.

Thus, despite the relatively small decrease in temperatures in ONtoOFF_grad compared to ON_ctrl (see Fig. 7), the cooler temperatures are the main driver of the evolution of the area of the different tree PFTs (TempNE, BoNE, BoBS) in the west of Western Europe.

These sensitivity runs also allow us to differentiate the roles of temperature and precipitation in the European vegetation temporal variability in ON_ctrl. In ONtoOFF_precip, ORCHIDEE is forced by the same climatic forcings as in ON_ctrl, except for precipitation, which allows us to evaluate the impact of a change in precipitation in the control run ON_ctrl. As mentioned above, Fig. 13 shows a similar evolution of areas occupied by BoNE and BoBS in ONtoOFF_precip compared to ON_ctrl, with nearly exactly the same interannual variability, including abrupt shifts for BoBS, which correspond to the brutal disappearance of the PFT over one or a few grid cells. Thus, a different pattern of precipitation does not affect the variability, which shows that the main driver of this variability is temperature. This is confirmed by the comparison of ON_ctrl with ONtoOFF_temp, which differs only for temperature and for which the evolution of BoNE and BoBS differs. However, the abrupt shifts cannot be linked to the mean annual temperature, the mean temperature of the coldest month, or the mean temperature of the warmest month of the years for which they occur (results not shown). The abrupt decreases could then be related either to temperatures at the daily timescale or, on the contrary, at longer timescale to temperatures during the years preceding the collapse. These two hypotheses have to be further investigated to better understand the cause of the instabilities in tree fractions.

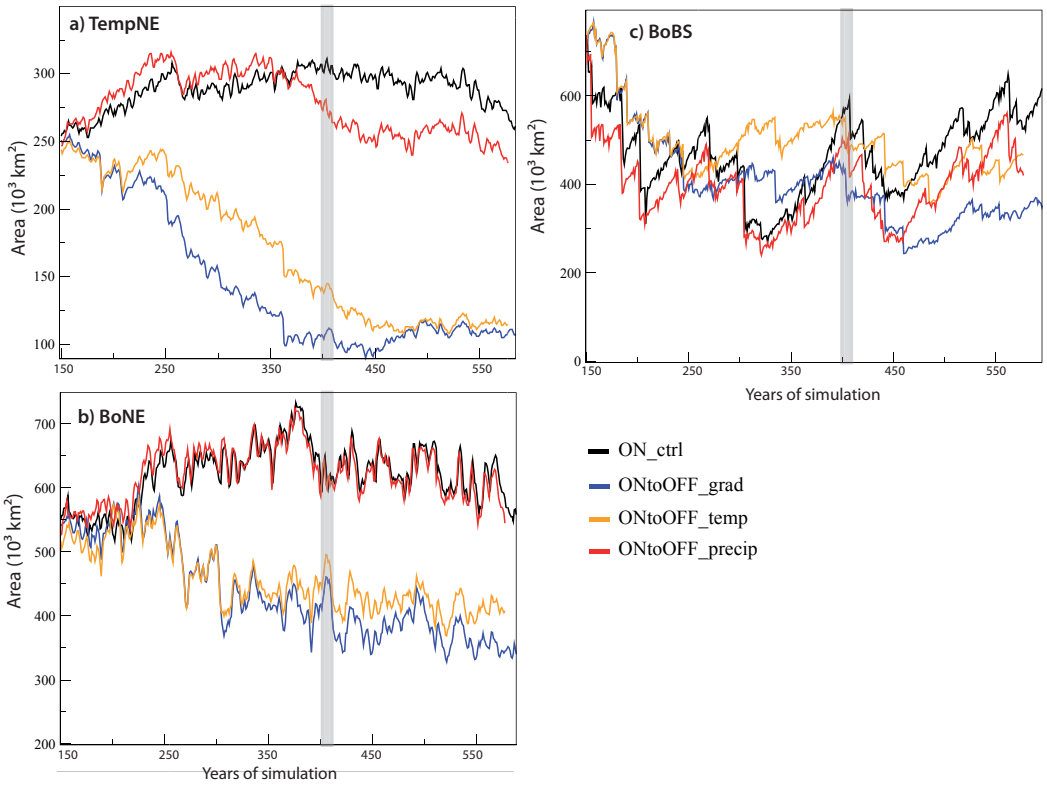

Fig. 13. Area of Western Europe (lat = 32/60°, lon = −15/20°) occupied by **(a)** Temperate needleleaf evergreen; **(b)** Boreal needleleaf evergreen; **(c)** Boreal broadleaf summergreen trees in ON_ctrl (black), ONtoOFF_grad (blue), ONtoOFF_precip (red) and ONtoOFF_temp (orange). The vertical grey bars indicate when the AMOC is fully collapsed in ONtoOFF_grad.

5.2.3 Recovery of the AMOC

When the AMOC gradually recovers (OFFtoON_grad), the forested area is back to the level of control values at the end of the run (Fig. 12a). However, contrary to the evolution of temperature and precipitation (Fig. 1b, c) no plateau is observed in the curve at the end of the run and the area covered by tree PFTs is probably not at equilibrium with the final climate of OFFtoON_grad, suggesting a lag of several decades between climate and vegetation. The area occupied by grass at the end of OFFtoON_grad (Fig. 12b) remains higher by about 100×10^3 km^2 than the mean level in ON_ctrl, but this value is within the range of variability of the control run.

When the climate is set back to the control state instantaneously (OFFtoON_inst), both forest and C3 grass areas are back to the levels of ON_ctrl within a century. This duration corresponds to the lag between climate and vegetation. We could have expected grass to respond faster than trees, but they actually reflect the evolution of forests and regress on areas where tree fractions increase.

The evolution of the areas covered by trees and grass in OFFtoON_fast, for which the AMOC jumps from 0 to 30 Sv within 150 yr, is quite similar to the one simulated in OFFtoON_inst. Final states are also similar, despite the very different AMOC strength. This result is not very surprising, given the limited impact of this high AMOC level on the climate of Western Europe compared to ON_ctrl (Figs. 1 and 2). However, the global results presented in Fig. 12 hides spatial differences in the area covered by the different PFTs. At the end of OFFtoON_fast compared to ON_ctrl, BoNE fractions are smaller over France, Germany and the North of Italy, replaced by BoBS and C3 grass. C3 grass extension decreases on the Atlantic French coast where BoBS and TempNE increase (results not shown). The change in climate at the end of OFFtoON_fast compared to ON_ctrl leads to a reorganisation of the distribution of the PFTs and modifications of the composition of forested areas, which are unseen in the evolution of the global forested area.

6 Discussion and conclusion

The main issues that we wanted to investigate in the present paper were: is the European glacial vegetation simulated by ORCHIDEE sensitive to AMOC changes? Can the model simulate vegetation changes in agreement with changes inferred from pollen data for HE or DO events? What is the timing of the vegetation evolution?

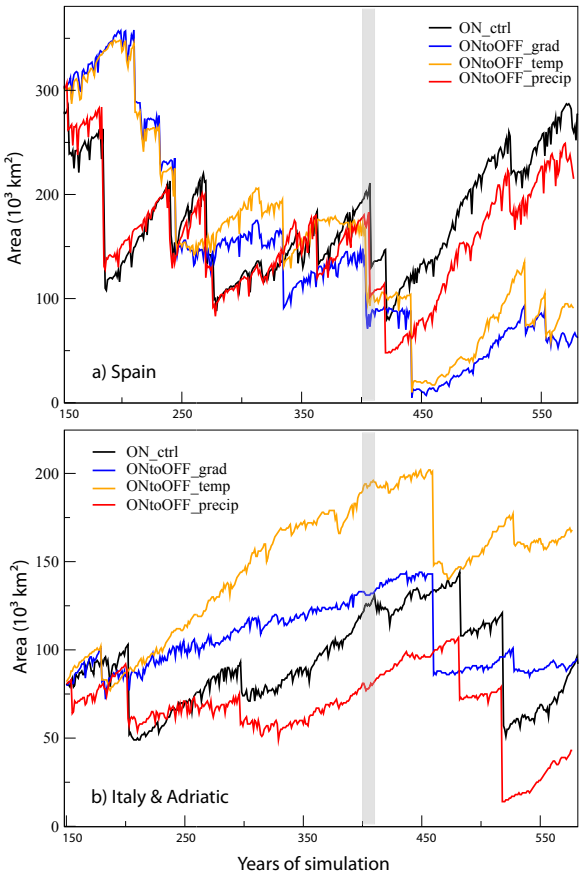

Fig. 14. Surface occupied by boreal broadleaf summergreen trees over **(a)** Spain and **(b)** Italy + Adriatic in ON_ctrl (black), ONtoOFF_grad (blue), ONtoOFF_precip (red) and ONtoOFF_temp (orange). The vertical grey bars indicate when the AMOC is fully collapsed in ONtoOFF_grad.

To investigate those questions, we have used the outputs of freshwater hosing experiments which have been performed under LGM conditions with the IPSL_CM4 AOGCM, to simulate a collapse and recovery of the AMOC at different rates. The different resulting climates have been used to drive the ORCHIDEE DGVM off-line and investigate the dynamical response of the glacial vegetation, with a special focus on the changes over Western Europe.

The glacial vegetation simulated by ORCHIDEE over Europe for the LGM control simulation, in which the AMOC is active, is characterised by an overestimated forest cover, consistent with the overestimation of temperature and precipitation over Western Europe in IPSL_CM4. The high forest fractions and the transition from broadleaf PFT in the south to needleleaf and then to grasses with increasing latitudes is more in agreement with pollen data for an interstadial than for the LGM. Our 1000 yr of LGM control simulation also shows a high interannual variability of the areas occupied by the boreal needleleaf evergreen and the boreal broadleaf summergreen trees. The glacial vegetation seems to be close to climatic thresholds and therefore very sensitive to climatic variability. Temperature seems to be the main driver of this variability, however further investigation is required to better understand the mechanism at play since no obvious correlation between annual or monthly temperature and the evolution of these two PFTs could be found.

When the AMOC collapses, IPSL_CM4 simulates the expected thermal bipolar see-saw between the two hemispheres, with cooling in the North Atlantic and warming in the Southern Ocean and a southward migration of the ITCZ. The opposite climatic response is simulated for the AMOC resumption. Temperature anomalies simulated over the North Atlantic do not propagate far inland over Western Europe because of the development of a cyclonic (resp. anticyclonic) anomaly which brings warm (resp. cool) air over the continent when the AMOC collapses (resp. recovers).

The climatic changes associated to an AMOC collapse lead to forests regression over Western Europe, replaced by grasses in qualitative agreement with pollen data for HE events. Sensitivity tests show that this European forest regression is mainly driven by the cooling in temperatures, although this cooling is limited to a few °C on average. For most parts of Western Europe, precipitation decrease appears to have only a small impact. Thus, our model vegetation is highly sensitive to temperature changes and a temperature decrease as strong as reconstructed from pollen data (e.g. Combourieu-Nebout et al., 2009b) is not required to drive important vegetation changes. This result suggests that the amplitude of climatic changes reconstructed from pollen data for HE events may be overestimated. However, the remaining simulated forest fractions simulated by ORCHIDEE at the end of the AMOC collapse are still overestimated over France compared to pollen data. Thus, even if climatic reconstructions may be biased, temperature and/or precipitation changes are probably nevertheless still underestimated by the AOGCM.

A more detailed statistical analysis of our results is required to better understand which temperature parameters drive the European vegetation changes. Is it an increase in the frequency of very cold temperatures at the daily scale? Or the long-term impact of temperature conditions less favourable, but not extreme? Another interesting point would be to investigate changes in the amplitude of the seasonal cycle, an important parameter for various Mediterranean and temperate species which is known to have changed during HE events in the western Mediterranean region (Combourieu-Nebout et al., 2009a).

The very limited impact of precipitation decrease in our vegetation simulations disagrees with reconstructions. As mentioned in Sect. 1, pollen data from the Iberian peninsula show an important development of xeric plants during HE events. Our results suggest an underestimation of the drying of climate in IPSL_CM5 or of its impact on the vegetation simulated by ORCHIDEE. However, xeric plants, such as *Artemisia*, are not explicitly simulated by ORCHIDEE.

The forest regression recorded in pollen data could indeed be driven by the temperature decrease and the development of xeric plants, among other types of grasses, favoured by the decrease in precipitation. A more complete description of the vegetation in ORCHIDEE would be needed to examine these hypotheses.

Our results on the timing of the vegetation response to AMOC changes are summarized in Fig. 15. The mean annual temperature (Fig. 15a) and the mean annual precipitation (Fig. 15b) both respond synchronously to AMOC changes. Both graphs show a large interannual variability of temperature and precipitation values for a given AMOC strength, but the relationship appears to be linear for AMOC values between 0 and 20 Sv. Temperature and precipitation values for AMOC strengths above 20 Sv are close to control values, showing the limited impact of a transient hyperactive AMOC on the European climate. The different values of forested areas in ONtoOFF_grad, OFFtoON_grad and OFFtoON_fast for AMOC strength between 7 and 12 Sv (Fig. 15c) clearly show a time lag between vegetation and AMOC changes. The total forested area being less variable than temperature and precipitation for a given AMOC strength, vegetation sensitivity to AMOC changes is also more visible. Given the synchronicity between the evolution of the AMOC and of the European climate, the time lag between the AMOC and vegetation is related to vegetation dynamics. We have shown that at the European scale this time lag is about 200 yr for an AMOC collapse and 100–200 yr for the AMOC recovery. The vegetation obtained for a very fast increase of the AMOC from 0 to 30 Sv is close to control state, partly because the simulation is not at equilibrium and partly because of the limited continental impact of this hyperactive AMOC.

The study of abrupt climatic events in marine cores from the Alboran Sea shows that the different DO and Heinrich events have very different signatures, both in the SST and in the pollen records (e.g. Fletcher and Sánchez-Goñi, 2008). The temporal resolution of the analyses carried out on the cores does not always allow a precise comparison of the timing of the ocean and vegetation response to abrupt events, and only few marine cores have a resolution good enough for such a comparison. The study of Sánchez-Goñi et al. (2002) shows a perfect coupling between terrestrial and marine changes for the Heinrich event 4 (H4) in the Alboran Sea, with a temporal resolution of 200 yr. The same study also shows that the timing of changes for two regions not so far from one another can be quite different: for H4, the maximum of steppic plants is reached at the onset of the event in the Alboran Sea, but only in the second part of the event on the Atlantic side of SW Iberia. Data from Combourieu-Nebout et al. (2009b), with a time resolution refined to 20–40 yr during abrupt events confirm the synchronicity between marine and terrestrial changes for HE events in the Alboran Sea. Other Atlantic and Mediterranean cores also record synchronous marine and continental changes for H2 (Combourieu-Nebout et al., 1998, 2002; Turon et al., 2003; Naughton et al., 2007).

The comparison of our results to pollen data can only be qualitative given the relatively coarse resolution of our model. Given the duration of our experiment, which is short compared to the time resolution of most of the available pollen records, our results for a collapse of the AMOC are in qualitative agreement with data for a Heinrich event. The rapidity of the vegetation response is also in agreement with the pollen record of Allen et al. (1999), showing vegetation changes occurring in less than 200 yr in the South of Italy. The lag of more than a century simulated when climatic conditions for an inactive AMOC are imposed instantaneously was somehow unexpected since trees can be killed within only a few years. This result suggests that the decrease of forest is driven by the succession of unfavourable years over a long period rather than by the abrupt crossing of a bioclimatic threshold. Besides, the amplitude of climate change reconstructed from pollen data for a Heinrich event is larger than the changes simulated by IPSL_CM4. A more drastic climate change would probably reduce the lag of simulated vegetation changes with respect to climate changes, which could be tested by adding systematic temperature and/or precipitation anomalies of different amplitudes to the forcing. Such an approach could allow for the establishment of a relationship between the amplitude of the climate change and the duration of the lag between climate and vegetation.

The time lag when the AMOC recovers could be expected since a forest obviously needs time to grow again, but this lag is much smaller than the several centuries needed for the regrowth of forests according to pollen data. In the south of Iberia (Alboran Sea site ODP 976) the forest maximum is reached 600 yr after the onset of DO 12 and 800 yr after the onset of DO 8. Vegetation changes in the Adriatic also occur over centuries, with about 400 to 1000 yr for the complete regrowth of forests after a minimum (N. Combourieu-Nebout, personal communication, 2012). This discrepancy might be related to the absence of simulation of pollen dispersal in the model. The regrowth of forests after a phase of severe regression first requires the transport of seeds at places where trees have disappeared. The dispersal of seeds from small remaining trees refugia might takes decades or century, depending on the distance between the refugia and the location considered (e.g. Brewer et al., 2002).

Another limitation of our study resides in the absence of feedbacks between the atmosphere and vegetation in our runs. Taking into account the increase in albedo, the reduction of evapotranspiration, and rugosity induced by the decrease of forests for an AMOC collapse would probably help to reach colder temperatures and to further reduce precipitation, which in return might reduce or suppress the time lag in the vegetation response. Similarly, the vegetation state resulting from the preceding cold phase might act as a negative feedback on the atmosphere and delay the return to warmer and wetter conditions, in particular through the snow albedo

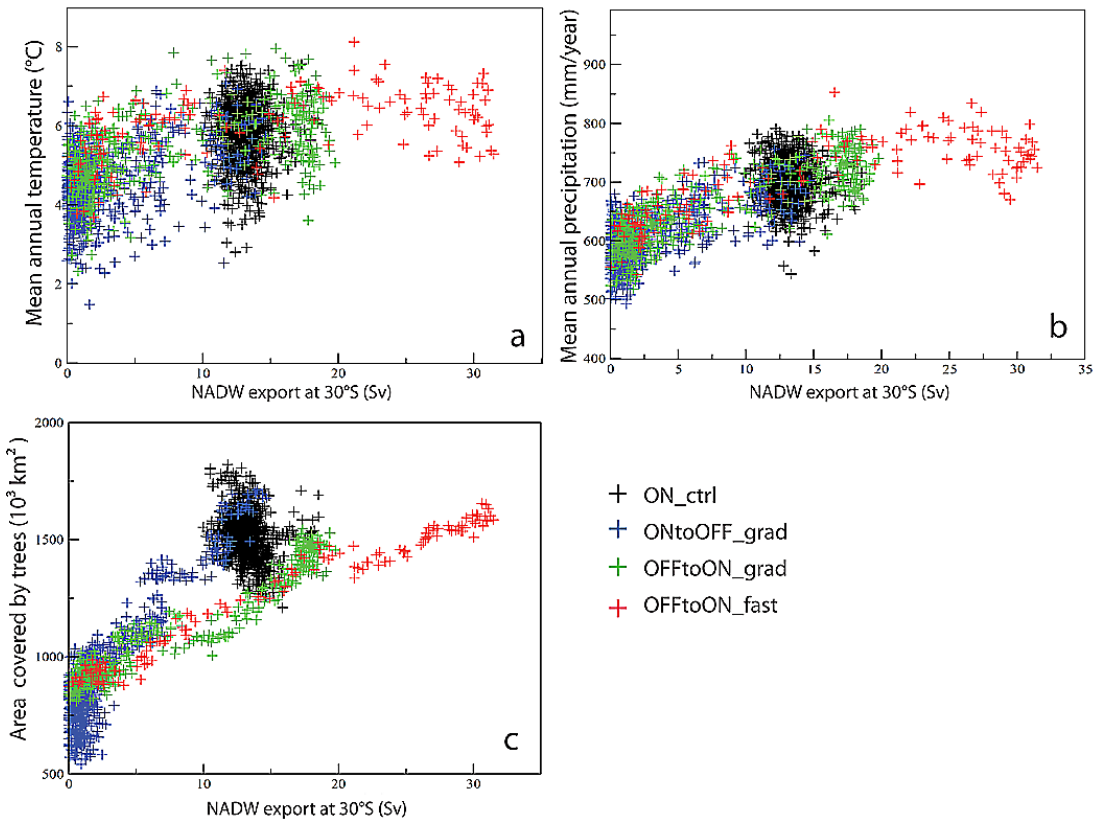

Fig. 15. (a) Mean annual temperature (°C), **(b)** mean annual precipitation (mm yr^{-1}) and **(c)** area covered by trees (10^3 km^2) over Western Europe (lat = 32/60°, lon = −15/20°) vs NADW strength at 30° S (Sv) for simulations ON_ctrl (black), ONtoOFF_grad (blue), OFFtoON_grad (green) and OFFtoON_fast (red). Each cross corresponds to the result for one year.

effect on regions where forests have disappeared. This hypothesis could be tested by comparing our present results to simulations with full coupling between climate and vegetation.

The response of European vegetation to a very fast shift in the AMOC strength from 0 to 30 Sv, designed to mimic a DO event, is very close to the response to an instantaneous return to the climatic conditions of the control run. Simulating an abrupt shift from a collapsed to a hyperactive AMOC is not necessary to qualitatively simulate the vegetation response to a DO, an abrupt return to initial conditions give the same results, which suggests that the equilibrium state of the glacial climate may correspond rather to interstadials than to stadials.

In any case, the disequilibrium between vegetation and climate during our transient simulations suggests that the assumption of vegetation-climate equilibrium used in palynological climate reconstructions may not be valid for time resolution higher than a century. To simulate vegetation changes in agreement with pollen data, different climatic scenarios are possible, depending on the existence and duration of a lag between climate and vegetation changes. Thus, the use of dynamic vegetation models can provide some constraints on abrupt changes on the continent, especially where pollen records are the only data available. Different rates and amplitudes of changes in temperature and precipitation can be tested to establish which scenarios can lead to vegetation changes in agreement with pollen data, for both the change in composition and the speed of change.

Acknowledgements. The simulations have been run on the computer of the Centre de Calcul Recherche et Technologie (CCRT, France). We thank two anonymous reviewers for their comments to improve this manuscript.

Edited by: F. Joos

The publication of this article is financed by CNRS-INSU.

References

Allen, J., Brandt, U., Brauer, A., Hubbertens, H.-W., Huntley, B., Keller, J., Kraml, M., Mackensen, A., Mingram, J., Negendank, J., Nowaczyk, N., Oberhänsli, H., Watts, W., Wulf, S., and Zolitschka, B.: Rapid environmental changes in southern europe during the last glacial period, Nature, 400, 740–743, 1999.

Alley, R. B., Anandakrishnan, S., and Jung, P.: Stochastic resonance in the North Atlantic, Paleoceanography, 16(2), 190–198, 2001.

Barker, S., Diz, P., Vautravers, M. J., Pike, J., Knorr, G., and Hall, I.: Interhemispheric atlantic seesaw response during the last deglaciation, Nature, 457, 1097–1103, 2009.

Berger, A.: Long-term variations of daily insolation and Quaternary climatic changes, J. Atmos. Sci., 35, 2362–2367, 1978.

Blunier, T., Chappellaz, J., Schwander, J., Dällenbach, A., Stauffer, B., Stocker, T., Raynaud, D., Jouzel, J., Clausen, H., Hammer, C., and Johnsen, S.: Asynchrony of Antarctic and Greenland climate change during the last glacial period, Nature, 394, 739–743, 1998.

Bond, G. and Lotti, R.: Iceberg Discharges into the North Atlantic on Millennial Time Scales During the Last Glaciation, Science, 267, 1005–1010, 1995.

Bozbiyik, A., Steinacher, M., Joos, F., Stocker, T. F., and Menviel, L.: Fingerprints of changes in the terrestrial carbon cycle in response to large reorganizations in ocean circulation, Clim. Past, 7, 319–338, doi:10.5194/cp-7-319-2011, 2011.

Braconnot, P., Otto-Bliesner, B., Harrison, S., Joussaume, S., Peterchmitt, J.-Y., Abe-Ouchi, A., Crucifix, M., Driesschaert, E., Fichefet, Th., Hewitt, C. D., Kageyama, M., Kitoh, A., Laîné, A., Loutre, M.-F., Marti, O., Merkel, U., Ramstein, G., Valdes, P., Weber, S. L., Yu, Y., and Zhao, Y.: Results of PMIP2 coupled simulations of the Mid-Holocene and Last Glacial Maximum – Part 1: experiments and large-scale features, Clim. Past, 3, 261–277, doi:10.5194/cp-3-261-2007, 2007.

Braun, H., Christl, M., Rahmstorf, S., Ganopolski, A., Mangini, A., Kubatzki, C., Roth, K., and Kromer, B.:Possible solar origin of the 1,470-year glacial climate cycle demonstrated in a coupled model, Nature, 438, 208–211, 2005.

Brewer, S., Cheddadi, R., de Beaulieu, J., Reille, M., and contributors, D.: The spread of deciduous *Quercus* throughout Europe since the last glacial period, Forest Ecol. Manage., 156, 27–48, 2002.

Claussen, M., Ganopolski, A., Brovkin, V., Gerstengarbe, F.-W., and Werner, P.: Simulated global-scale response of the climate system to Dansgaard/Oeschger and Heinrich events, Clim. Dynam., 21, 361–370, 2003.

Clement, A. and Peterson, L.: Mechanisms of abrupt climate change of the last glacial period, Rev. Geophys., 46, RG4002, doi:10.1029/2006RG000204, 2008.

Combourieu-Nebout, N., Paterne, M., Turon, J.-L., and Siani, G.: A high-resolution record of the last deglaciation in the central Mediterranean Sea: palaeovegetation and palaeohydrological evolution, Quaternary Sci. Res., 17, 303–317, 1998.

Combourieu-Nebout, N., Turon, J.-L., Zahn, R., Capotondi, L., Londeix, L., and Pahnke, K.: Enhanced aridity and atmospheric high-pressure stability over the western Mediterranean during the North Atlantic cold events of the past 50 k.y., Geology, 30, 863–866, 2002.

Combourieu-Nebout, N., Bout-Roumazeilles, V., Dormoy, I., and Peyron, O.: Persistent dryness events in the mediterranean along the last 50 000 years, Sécheresse, 20, 210–216, 2009a.

Combourieu-Nebout, N., Peyron, O., Dormoy, I., Desprat, S., Beaudouin, C., Kotthoff, U., and Marret, F.: Rapid climatic variability in the west Mediterranean during the last 25 000 years from high resolution pollen data, Clim. Past, 5, 503–521, doi:10.5194/cp-5-503-2009, 2009b.

Crowley, T.: North Atlantic deep waters cools the southern hemisphere, Paleoceanography, 7, 489–497, 1992.

Dällenbach, A., Blunier, T., Flückiger, J., Stauffer, B., Chappellaz, J., and Raynaud, D.: Changes in the atmospheric CH4 gradient between Grennland and Antartica during the Last Glacial and the transition to the Holocene, Geophys. Res. Lett., 27, 1005–1008, 2000.

Dansgaard, W., Johnson, S., Clausen, H., Dahl-Jensen, D., Gundestrup, N., Hammer, C., Hvidberg, C., Steffensen, J., Sveinbjornsdottir, A., and Jouzel, J.: Evidence for general instabilities of past climate from a 250-kyr ice-core record, Nature, 364, 218–220, 1993.

de Beaulieu, J. and Reille, M.: A long Upper Pleistocene pollen record from Les Echets, near Lyon, France, Boreas, 13, 111–132, 1984.

de Beaulieu, J. and Reille, M.: Long Pleistocene pollen sequences from the Velay Plateau (Massif Central, France), Veg. Hist. Archaeobot., 1, 233–242, 1992a.

de Beaulieu, J. and Reille, M.: The last climatic cycle at La Grande Pile (Vosges, France) a new pollen profile, Quaternary Sci. Res., 11, 431–438, 1992b.

Ditlevsen, P. D., Andersen, K. K., and Svensson, A.: The DO-climate events are probably noise induced: statistical investigation of the claimed 1470 years cycle, Clim. Past, 3, 129–134, doi:10.5194/cp-3-129-2007, 2007.

Elliot, M., Labeyrie, L., and Duplessy, J.-C.: Changes in North Atlantic deep-water formation associated with the Dansgaard-Oeschger temperature oscillations (60–10 ka), Quaternary Sci. Res., 21, 1153–1165, 2002.

EPICA Community Members: One-to-one coupling of glacial climate variability in Greenland and Antarctica,Nature, 444, 195–198, 2006.

Fletcher, W. and Sánchez-Goñi, M.-F.: Orbital- and sub-orbital-scale climate impacts on vegetation of the western Mediterranean basin over the last 48,000 years, Quaternary Res., 70, 451–464, 2008.

Fletcher, W., Sánchez-Goñi, M. F., Allen, J., Cheddadi, R., Combourieu-Nebout, N., Huntley, B., Lawson, I., Londeix, L., Magri, D., Margari, V., Müller, U., Naughton, F., Novenko, E., Roucoux, K., and Tzedakis, P.: Millennial-scale variability during the last glacial in vegetation records from Europe, Quat. Scie. Rev., 29, 2839–2864, 2010.

Flückiger, J., Dällenbach, A., Blunier, T., Stauffer, B., Stocker, T., Raynaud, D., and Barnola, J.: Variations in atmospheric N_2O concentration during abrupt climatic changes, Science, 285, 227–230, 1999.

Ganopolski, A. and Rahmstorf, S.: Rapid changes of glacial climate simulated in a coupled climate model, Nature, 409, 153–158, 2001.

Grimm, E., Watts, W., Jacobson, G., Hansen, B., Halmquist, H., and Dieffenbacher-Krall, A.: Evidence for warm wet Heinrich events in Florida, Quaternary Sci. Res., 25, 2197–2211, (2006).

Guiot, J.: Methodology of the last climatic reconstruction in France from pollen data, Palaeogeogr. Palaeocl., 80, 49–69, 1990.

Heinrich, H.: Origin and consequences of cyclic ice rafting in the northeast Atlantic ocean during the past 130,000 years, Quaternary Res., 29, 142–152, 1988.

Hessler, I., Dupont, L., Bonnefille, R., Behling, H., González, C., Helmens, K., Hooghiemstra, H., Lebamba, J., Ledru, M.-P., Lézine, A.-M., Maley, J., Marret, F., and Vincens, A.:Millennial-scale changes in vegetation records from tropical Africa and South America during the last glacial, Quaternary Sci. Res., 29, 2882–2899, 2010.

Hu, A., Otto-Bliesner, B., Meehl, G., Han, W., Morrill, C., Brady, E., and Briegleb, B.: Response of Thermohaline Circulation to Freshwater Forcing under Present-Day and LGM Conditions, J. Climate, 21, 2239–2258, 2008.

Johnsen, S., Clausen, H., Dansgaard, W., Fuhrert, K., Gundestrup, N., Hammer, C., Iversen, P., Jouzel, J., Stauffer, B., and Steffensen, J.: Irregular glacial interstadials recorded in a new Greenland ice core, Nature, 359, 311–313, 1992.

Johnsen, S., Dahl-Jensen, D., Dansgaard, W., and Gundestrup, N.: Greenland paleotemperatures derived from GRIP bore hole temperature and ice core isotope profiles, Tellus, 47B, 624–629, 1995.

Jouzel, J., Vimeux, F., Caillon, N., Delaygue, G., Hoffmann, G., Masson-Delmotte, V., and Parrenin, F.: Magnitude of isotope/temperature scaling for interpretation of central Antarctic ice cores, J. Geophys. Res., 108, D124361, doi:10.1029/2002JD002677, 2003.

Kageyama, M., Combourieu Nebout, N., Sepulchre, P., Peyron, O., Krinner, G., Ramstein, G., and Cazet, J.: The Last Glacial Maximum and Heinrich event 1 in terms of climate and vegetation around the Alboran sea: a preliminary model-data comparison, C. R. Geosci., 337, 938–992, 2005.

Kageyama, M., Mignot, J., Swingedouw, D., Marzin, C., Alkama, R., and Marti, O.: Glacial climate sensitivity to different states of the Atlantic Meridional Overturning Circulation: results from the IPSL model, Clim. Past, 5, 551–570, doi:10.5194/cp-5-551-2009, 2009.

Kageyama, M., Paul, A., Roche, D., and Van Meerbeeck, C.: Modelling glacial climatic millenial-scale variability related to changes in the Atlantic meridional overturning circulation: a review, Quaternary Sci. Rev., 29, 2931–2956, 2010.

Köhler, P., Joos, F., Gerber, S., and Knutti, R.: Simulated changes in vegetation distribution, land carbon storage, and atmospheric CO_2 in response to a collapse of the North Atlantic thermohaline circulation, Clim. Dynam., 25, 689–708, 2005.

Krinner, G., Viovy, N., de Noblet-Ducoudré, N., Ogée, J., Polcher, J., Friedlingstein, P., Ciais, P., Sitch, S., and Prentice, I. C.: A dynamic global vegetation model for studies of the coupled atmosphere-biosphere system, Global Biogeochem. Cy., 19, GB1015, doi:10.1029/2003GB002199, 2005.

Landais, A., Caillon, N., Goujon, C., Grachev, A., Barnola, J., Chappellaz, J., Jouzel, J., Masson-Delmotte, V., and Leuenberger, M.: Quantification of rapid temperature change during DO event 12 and phasing with methane inferred from air isotopic measurements, Earth Planet. Sci. Lett., 225, 221–232, 2004.

Manabe, S. and Stouffer, R.: Simulation of abrupt climate change induced by freshwater input to the North Atlantic Ocean, Nature, 378, 165–167, 1995.

Marti, O., Braconnot, P., Dufresne, J., Bellier, J., Benshila, R., Bony, S., Brockmann, P., Cadule, P., Caubel, A., Codron, F., de Noblet, N., Denvil, S., Fairhead, L., Fichefet, T., Foujols, M., Friedlingstein, P., Goosse, H., Granpeix, J., Guilyardi, E., Hourdin, F., Idelkadi, A., Kageyama, M., Krinner, G., Levy, C., Madec, G., Mignot, J., Musat, I., Swingedouw, D., and Talandier, C.: Key features of the IPSL ocean atmosphere model and its sensitivity to atmospheric resolution, Clim. Dynam., 34, 1–26, 2010.

McManus, J., Francois, R., Gherardi, J.-M., Keigwin, L., and Brown-Leger, S.: Collapse and rapid resumption of atlantic meridional circulation linked to deglacial climate changes, Nature, 428, 834–837, 2004.

Menviel, L., Timmermann, A., Mouchet, A., and Timm, O.: Meridional reorganizations of marine and terrestrial productivity during Heinrich events, Paleoceanography, 23, PA1203, doi:10.1029/2007PA001445, 2008.

Monnin, E., Indermuhle, A., Dallenbach, A., Fluckiger, J., Stauffer, B., Stocker, T., Raynaud, D., and Barnola, J.: Atmospheric CO_2 concentrations over the last glacial termination, Science, 291, 112–114, 2001.

Naughton, F., Sánchez-Goñi, M.-F., Desprat, S., Turon, J.-L., Duprat, J., Malaizé, B., Joli, C., Cortijo, E., Drago, T., and Freitas, M.:Present-day and past (last 25 000 years) marine pollen signal off western Iberia,Mar. Micropaleontol., 62, 91–114, 2007.

Otto-Bliesner, B. and Brady, C.: The sensitivity of the climate response to the magnitude and location of freshwater forcing: last glacial maximum experiments, Quaternary Sci. Res., 29, 56–73, 2010.

Peltier, W.: Global glaacial isostasy and the surface of the ice-age Earth: the ICE-5G (VM2) Model and GRACE, Ann. Rev. Earth Planet. Sc., 32, 111–149, 2004.

Piotrowski, A., Goldstein, S., Hemming, S., and Fairbanks, R.: Temporal relationships of carbon cycling and ocean circulation at glacial boundaries, Science, 307, 1933–1938, 2005.

Prentice, I., Jolly, D., and BIOME 6000 participants: Mid-Holocene and glacial-maximum vegetation geography of the northern continents and Africa, J. Biogeogr., 27, 507–519, 2000.

Reille, M. and de Beaulieu, J.: History of the Würm and Holocene vegetation in the Western Velay (Massif Central, France): a comparison of pollen analysis from three corings at Lac du Bouchet, Rev. Palaeobot. Palyno., 54, 233–248, 1988.

Reille, M. and de Beaulieu, J.: Pollen analysis of a long Upper Pleistocene continental sequence in a Velay maar (Massif Central, France), Palaeogeogr. Palaeocl., 80, 35–48, 1990.

Roucoux, K., de Abreu, L., Shackleton, N., and Tzedakis, P.: The response of NW Iberian vegetation to North Atlantic climate oscillations during the last 65 kyr, Quaternary Sci. Res., 24, 1637–1653, 2005.

Sánchez-Goñi, M.-F., Cacho, I., Turon, J.-L., Guiot, J., Sierro, F. J., Peypouquet, J.-P., Grimalt, J. O., and Shackleton, N. J.: Synchroneity between marine and terrestrial responses to millennial scale climatic variability during the last glacial period in the Mediterranean region, Clim. Dynam., 19, 95–105, 2002.

Sánchez-Goñi, M.-F., Landais, A., Fletcher, W., Naughton, F., Desprat, S., and Duprat, J.: Contrasting impacts of Dansgaard-Oeschger events over a western European latitudinal transect modulated by orbital parameters, Quaternary Sci. Res., 27, 1136–1151, 2008.

Scholze, M., Knorr, W., and Heimann, M.: Modelling terrestrial vegetation dynamics and carbon cycling for an abrupt climatic change event, The Holocene, 13, 327–333, 2003.

Schulz, M.: On the 1470-year pacing of Dansgaard-Oeschger warm events, Paleoceanography, 17, 1014, doi:10.1029/2000PA000571, 2002.

Sitch, S., Smith, B., Prentice, I., Arneth, A., Bondeau, A., Cramer, W., Kaplan, J., Levis, S., Lucht, W., Sykes, M., Thonicke, K., and Venevsky, S.: Evaluation of ecosystem dynamics, plant geography and terrestrial carbon cycling in the LPJ dynamic global vegetation model, Glob. Change Biol., 9, 161–185, 2003.

Stocker, S. and Johnsen, S.: A minimum thermodynamic model for the bipolar seesaw, Paleoceanography, 18, 1087, doi:10.1029/2003PA000920, 2003.

Tjallingii, R., Claussen, M., Stuut, J.-B. W., Fohlmeister, J., Jahn, A., Bickert, T., Lamy, F., and Röhl, U.: Coherent high- and low-latitude control of the northwest african hydrological balance, Nat. Geosci., 1, 670–675, 2008.

Turon, J.-L., Lézine, A.-M., and Denèfle, M.: Land-sea correlations for the last glaciation inferred from a pollen and dynocist record from the Portiguese margin, Quaternary Res., 59, 88–96, 2003.

Voelker, A.: Global distribution of centennial-scale records for marine isotope stage (MIS) 3: a database, Quaternary Sci. Res., 21, 1185–1212, 2002.

Woillard, G.: Grande Pile peat bog: a continuous pollen record for the last 140,000 years, Quaternary Res., 9, 1–21, 1978.

Woillez, M.-N.: Modélisation des variations climatiques rapides du système atmosphère-ocan-végétation-cryosphère en climats glaciaires, Ph.D. thesis, Université de Versailles Saint-Quentin-en-Yvelines, 2012.

Woillez, M.-N., Kageyama, M., Krinner, G., de Noblet-Ducoudré, N., Viovy, N., and Mancip, M.: Impact of CO_2 and climate on the Last Glacial Maximum vegetation: results from the ORCHIDEE/IPSL models, Clim. Past, 7, 557–577, doi:10.5194/cp-7-557-2011, 2011.

Woillez, M.-N., Krinner, G., Kageyama, M., and Delaygue, G.: Impact of solar forcing on the surface mass balance of northern ice sheets for glacial conditions, Earth Planet. Sci. Lett., 335–336, 18–24, 2012.

Wolff, E., Chappellaz, J., Blunier, T., Rasmussen, S., and Svensson, A.: Millenial-scale variability during the last glacial: The ice core record, Quaternary Sci. Res., 29, 2828–2838, 2010.

Wu, H., Guiot, J., Brewer, S., and Guo, Z.: Climatic changes in Eurasia and Africa at the last glacial maximum and mid-Holocene: reconstruction from pollen data using inverse vegetation modelling, Clim. Dynam., 29, 211–229, 2007.